北京应用物理与计算数学研究所
IAPCM Institute of Applied Physics and Computational Mathematics

IWLS 2026，ZJU

Characteristics of shock waves and hydrodynamic instabilities in high-energy density plasmas

Hongbo Cai, Xu Zhang, Fanqi Meng, Mingjun Chen, Hanxiao Huang, Wenshuai Zhang, Shaoping Zhu

[1] Graduate School of China Academy of Engineering Physics
[2] Institute of Applied Physics and Computational Mathematics
[3] School of Physics, Zhejiang University

Outline

- **Development of Hybrid fluid-PIC code for ICF**
- **Characteristics of shock waves in HED plasmas**
- **Characteristics of hydrodynamic instabilities in HDP plasmas**

Typical hydrodynamic instabilities (HI) in ICF

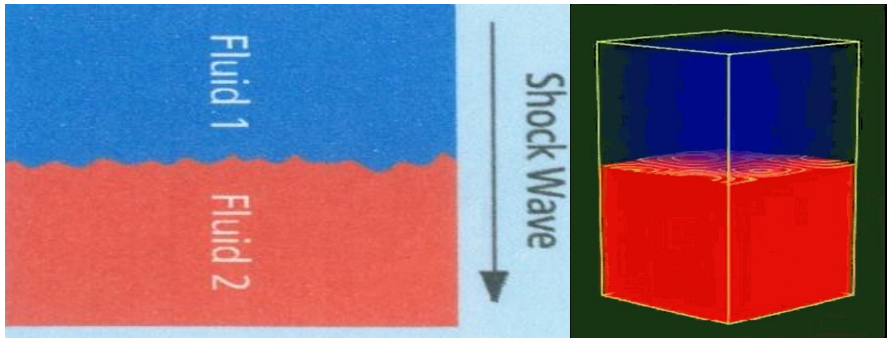

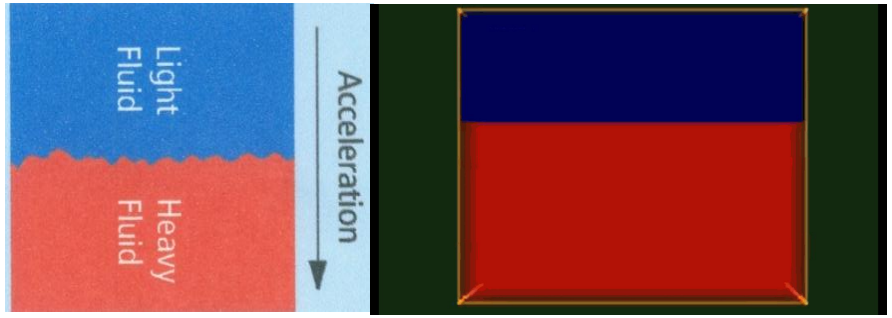

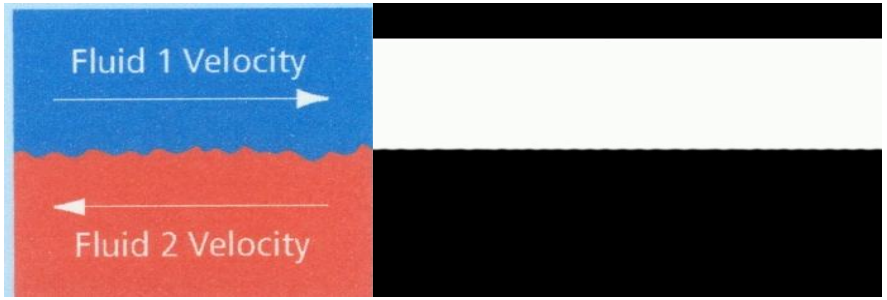

• In ICF, there are three typical hydrodynamic instabilities:

1. Richtmyer-Meshkov (RM) instability:
Impulsive acceleration; shock + perturbed interface

2. Rayleigh-Taylor (RT) instability:
Results from constant acceleration (A lighter fluid is accelerated into a heavier fluid)

3. Kelvin-Helmholtz (KH) instability:
Results from sheared velocity flow

The development of hydrodynamic instabilities result in the ion mixing at the interface, which increases the radiative cooling and severely degrades the performance of ICF.

It is crucially important to model HI and ion mixing in ICF self-consistently.

Characteristics of hydrodynamic instabilities in plasma

The vorticity equation: describe the structure and evolution of the HI

$$\frac{d\,\boldsymbol{\omega}}{d\,t} = \frac{\nabla\,\rho \times \nabla\,p}{\rho^{2}} + \boldsymbol{\omega}\cdot\nabla\,\mathbf{u} - \boldsymbol{\omega}\,\nabla\cdot\mathbf{u} \qquad (1)$$

0 in 2D

Vorticity: $\boldsymbol{\omega} = \nabla \times \mathbf{u}$

Baroclinic term　　Stretching term　　Compression term

Equation for self-generated magnetic field in plasmas

$$\frac{\partial \mathbf{B}}{\partial t} = \nabla \times (\mathbf{V} \times \mathbf{B}) - \nabla \times \left(\frac{\mathbf{J}}{en_e} \times \mathbf{B}\right) + \frac{c}{m_\alpha n_e^{\,2}} \nabla\rho \times \nabla p_e - c\nabla \times \left(\frac{\mathbf{R}_T}{en_e}\right) - c\nabla \times \left(\eta_{\parallel}\mathbf{J}_{\parallel} + \eta_{\perp}\mathbf{J}_{\perp}\right) \qquad (2)$$

Biermann battery effect　　阻尼扩散项

- In a plasma, the Biermann battery source term of the magnetic field is consistent with the baroclinic term of the vorticity. Thus, the magnetic field grows as the development of the HI.

hydrodynamic instabilities in plasmas: Problem 1

- During the ICF implosion, Te > 100eV (~1MK) , the capsule target becomes fully ionized plasma.
- During the evolution of the hydrodynamic instabilities(HI), the MG B-field and ion mixing are developed.
- How do the B-field and ion mixing affect the evolution of the HI and implosion performance in ICF?（**Problem 1**）

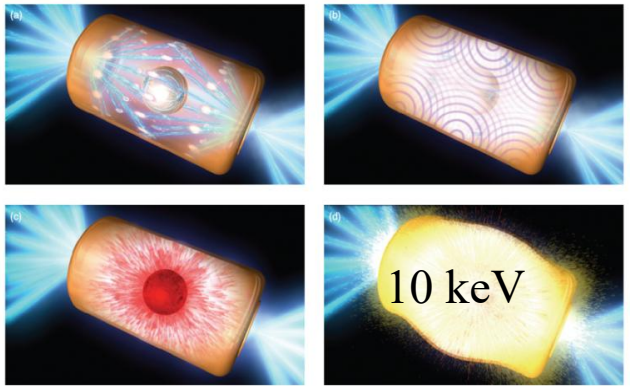

ICF implosion

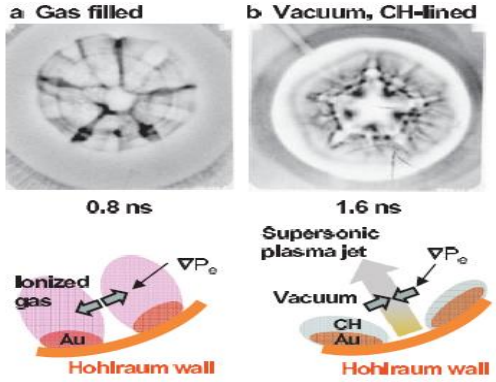

[1] C.K. Li, PRL (2012).

ICF hohlraum (MG B-field)

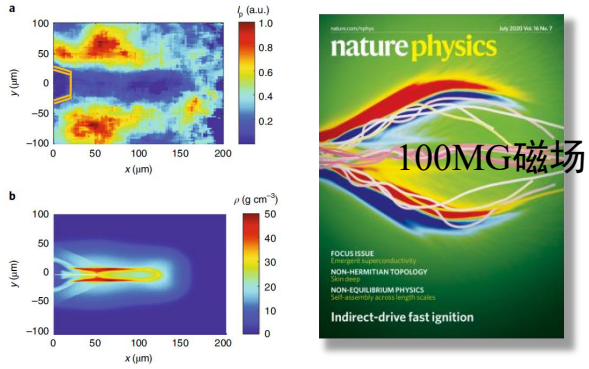

[2] F. Zhang# et al., Nature Physics (2020)

Implosion: 100MG B-field

Radiation hydrodynamic code

$$\frac{d\vec{u}}{dt} = -\frac{1}{\rho}\nabla(p_e + p_i + p_r + q)$$

$$\frac{d(C_{ve}T_e + V)}{dt} = -\frac{1}{\rho}\nabla\cdot\vec{F}_e - p_e\frac{d}{dt}\left(\frac{1}{\rho}\right) + W_{ie} + W_l - W_r$$

$$\frac{d(C_{vi}T_i)}{dt} = -\frac{1}{\rho}\nabla\cdot\vec{F}_i - p_i\frac{d}{dt}\left(\frac{1}{\rho}\right) - W_{ie}$$

No magnetic model
No ion mixing model

Research Methods

	Collisional	Transition region	collisionless
density	$>10^{23}cm^{-3}$		$<10^{21}cm^{-3}$
Knudsen number $Kn=\lambda_{ii}/L$	$< 10^{-2}$		$> 10^{0}$
Simulation tool	**Hydrodynamic code**	**Hybrid fluid-PIC code**	**PIC/Vlasov code**

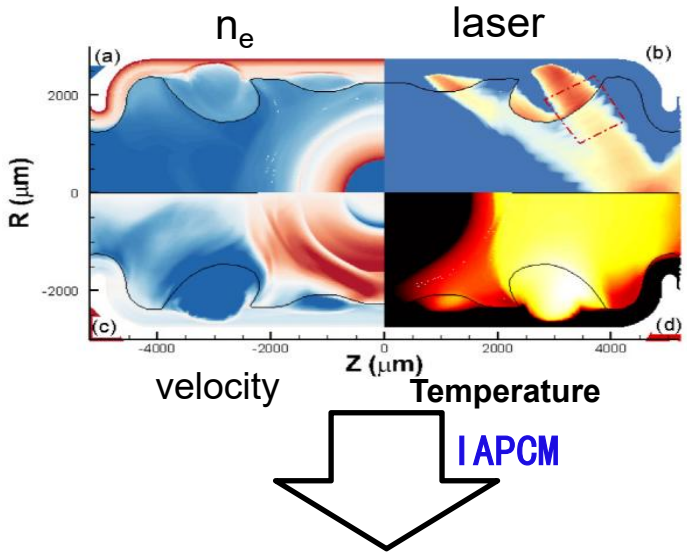

Characteristics It can simulate whole ICF processes (~10ns), but it can not self-consistently consider the ion mixing, penetration, and other kinetic effects, e.g. electric field

Physical modeling precision

Research Methods

	Collisional	Transition region	collisionless
density	$>10^{23}cm^{-3}$		$<10^{21}cm^{-3}$

Knudsen number $Kn=\lambda_{ii}/L$: $< 10^{-2}$ ... $> 10^{0}$

	Collisional	Transition region	collisionless
Simulation tool	Hydrodynamic code	Hybrid fluid-PIC code	PIC/Vlasov code

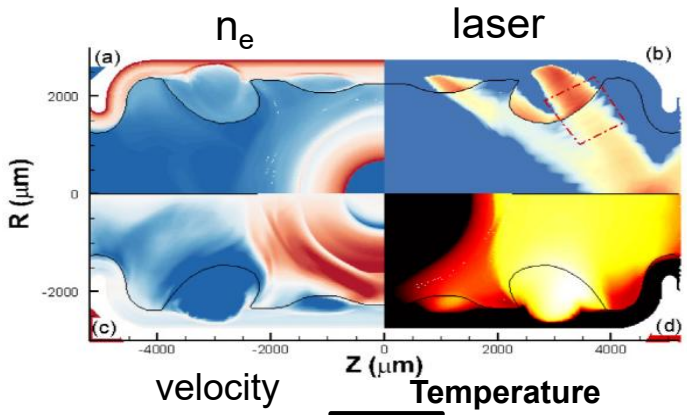

IAPCM

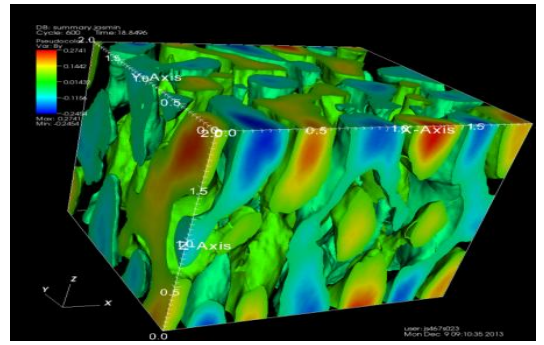

Characteristics It can simulate the kinetic processes, but its spatio-temporal simulation capability is limited in ICF (~ps, ~100μm) , which is not suitable for hydrodynamic instabilities.

Physical modeling precision

Research Methods

	Collisional	Transition region	collisionless
density	$>10^{23}cm^{-3}$		$<10^{21}cm^{-3}$
Knudsen number $Kn=\lambda_{ii}/L$	**< 10^{-2}**		**> 10^{0}**
Simulation tool	**Hydrodynamic code**	**Hybrid fluid-PIC code**	**PIC/Vlasov code**

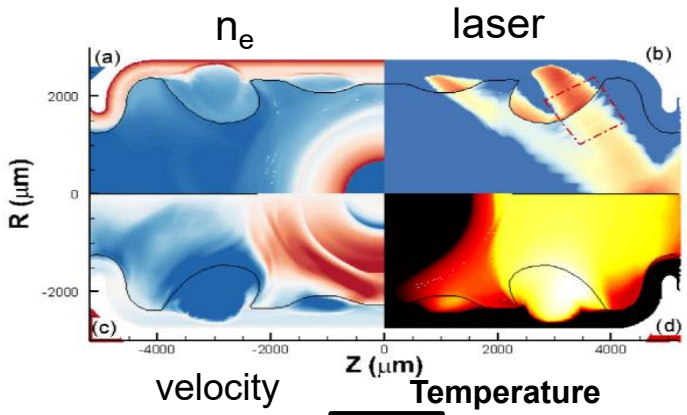

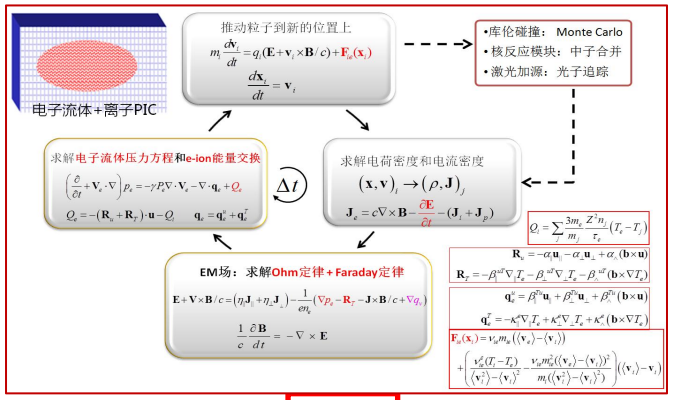

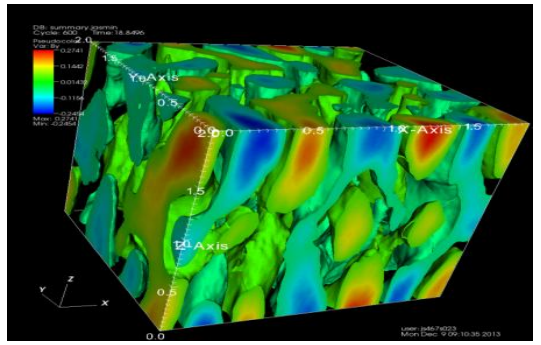

IAPCM

Ascent-Hybrid

Requirement Balancing fluid and kinetic simulation characteristics. The code can simulate ion mixing and penetration, and hydrodynamic instabilities in ns-level.

Physical modeling precision

Physical modeling of hybrid fluid-PIC code

Requirement: The code can simulate plasma penetration, hydrodynamic instabilities and ion mixing

Model

- **Electron:** modeled as a massless fluid, solve MHD equation (no electron fluctuation)
- **Ion:** modeled using the standard PIC method (keep the non-equilibrium ions)
- **EM field:** Ohm's law + Faraday's law
- **Fluid :** solve continuity eq., electron pressure eq., consider energy transfer between fluid-e and ions

Merit

dt relax significantly, $\mathrm{dt}\sim\frac{1}{\omega_{pi}}\sim\sqrt{\frac{m_i}{m_e}}\frac{1}{\omega_{pe}}$, no longer limited by Debye length

➔ simulation time increases 100 times longer (10 ps ➔ ns)

Hybrid fluid-PIC code: Ascent-hybrid = **MHD code** + **Ions: PIC method**

Physical modeling of hybrid fluid-PIC code: Ascent-H

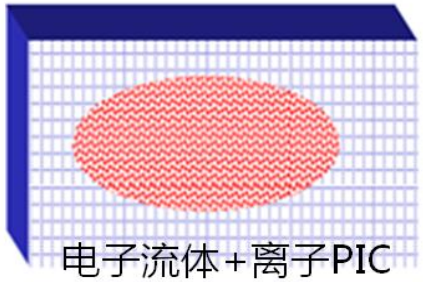

推动粒子到新的位置上

$$m_i \frac{d\mathbf{v}_i}{dt} = q_i(\mathbf{E}+\mathbf{v}_i\times\mathbf{B}/c)+\mathbf{F}_{ie}(\mathbf{x}_i)$$

$$\frac{d\mathbf{x}_i}{dt} = \mathbf{v}_i$$

- 库伦碰撞： Monte Carlo
- 核反应模块：中子合并
- 激光加源：光子追踪

difficulty

求解电子流体压力方程和e-ion能量交换

$$\left(\frac{\partial}{\partial t}+\mathbf{V}_e\cdot\nabla\right)p_e = -\gamma P_e\nabla\cdot\mathbf{V}_e-\nabla\cdot\mathbf{q}_e+Q_e$$

$$Q_e = -(\mathbf{R}_u+\mathbf{R}_T)\cdot\mathbf{u}-Q_i \qquad \mathbf{q}_e = \mathbf{q}_e^u+\mathbf{q}_e^T$$

Δt

求解电荷密度和电流密度

$$(\mathbf{x},\mathbf{v})_i \rightarrow (\rho,\mathbf{J})_j$$

$$\mathbf{J}_e = c\nabla\times\mathbf{B}-\frac{\partial\mathbf{E}}{\partial t}-(\mathbf{J}_i+\mathbf{J}_p)$$

EM场： 求解Ohm定律+Faraday定律

$$\mathbf{E}+\mathbf{V}\times\mathbf{B}/c = \left(\eta_{\parallel}\mathbf{J}_{\parallel}+\eta_{\perp}\mathbf{J}_{\perp}\right)-\frac{1}{en_e}\left(\nabla p_e-\mathbf{R}_T-\mathbf{J}\times\mathbf{B}/c+\nabla q_v\right)$$

$$\frac{1}{c}\frac{\partial\mathbf{B}}{dt} = -\nabla\times\mathbf{E}$$

$$Q_i = \sum_j \frac{3m_e}{m_j}\frac{Z^2 n_j}{\tau_e}(T_e-T_j)$$

$$\mathbf{R}_u = -\alpha_{\parallel}\mathbf{u}_{\parallel}-\alpha_{\perp}\mathbf{u}_{\perp}+\alpha_{\wedge}(\mathbf{b}\times\mathbf{u})$$

$$\mathbf{R}_T = -\beta_{\parallel}^{uT}\nabla_{\parallel}T_e-\beta_{\perp}^{uT}\nabla_{\perp}T_e-\beta_{\wedge}^{uT}(\mathbf{b}\times\nabla T_e)$$

$$\mathbf{q}_e^u = \beta_{\parallel}^{Tu}\mathbf{u}_{\parallel}+\beta_{\perp}^{Tu}\mathbf{u}_{\perp}+\beta_{\wedge}^{Tu}(\mathbf{b}\times\mathbf{u})$$

$$\mathbf{q}_e^T = -\kappa_{\parallel}^e\nabla_{\parallel}T_e+\kappa_{\perp}^e\nabla_{\perp}T_e+\kappa_{\wedge}^e(\mathbf{b}\times\nabla T_e)$$

$$\mathbf{F}_{ie}(\mathbf{x}_i) = \nu_{ie}m_{ie}\left(\langle\mathbf{v}_e\rangle-\langle\mathbf{v}_i\rangle\right)+\left(\frac{\nu_{ie}^{\varepsilon}(T_i-T_e)}{\langle\mathbf{v}_i^2\rangle-\langle\mathbf{v}_i\rangle^2}-\frac{\nu_{ie}m_{ie}^2(\langle\mathbf{v}_e\rangle-\langle\mathbf{v}_i\rangle)^2}{m_i(\langle\mathbf{v}_i^2\rangle-\langle\mathbf{v}_i\rangle^2)}\right)(\langle\mathbf{v}_i\rangle-\mathbf{v}_i)$$

[1] Hongbo Cai* et al., Matter Radiat. Extremes 6, 035901 (2021)

Verification: Formation and propagation of shock waves in plasma

- **Ascent-Hybrid**: Balancing macroscopic spatiotemporal evolution and microscopic details of ion kinetic effects
- The kinetic effects of ions in shock waves are significant: upstream, ion reflection; while downstream, ion trapping

t=400 ps

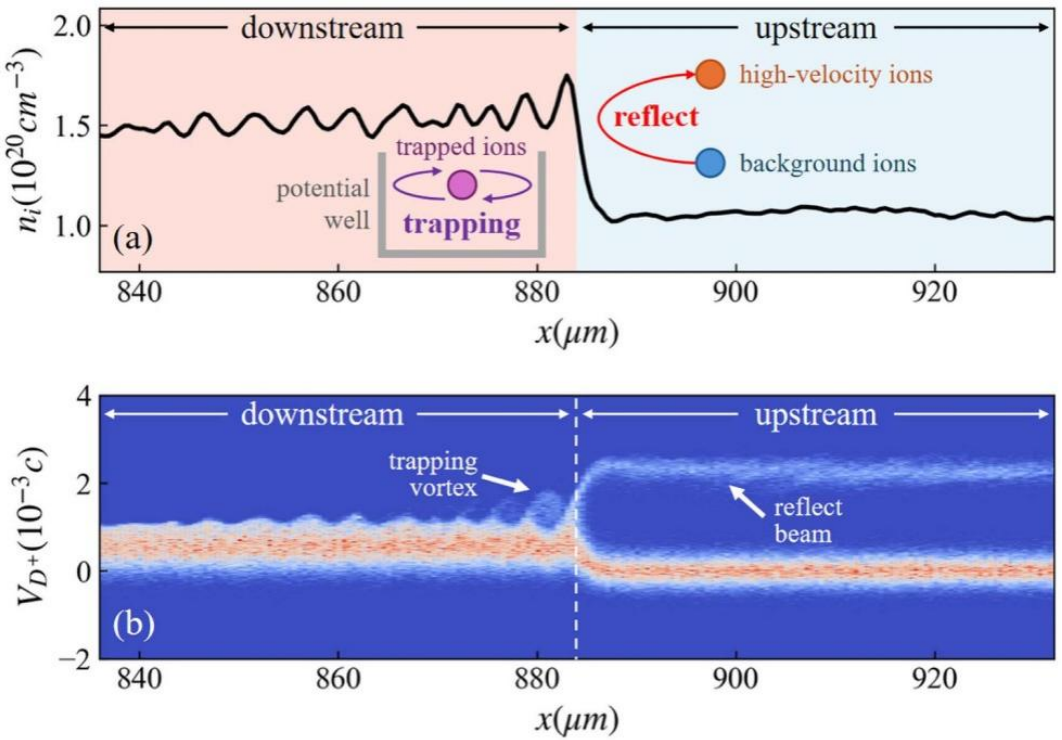

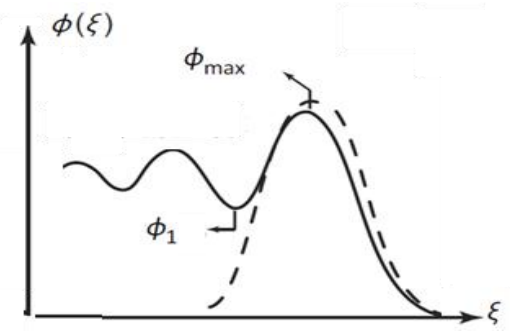

(a) Schematic diagram of solitary waves and shock wave structures

$$\rho_1 u_1 = \rho_2 u_2,$$
$$\rho_1 u_1^2 + p_1 = \rho_2 u_2^2 + p_2,$$
$$\frac{u_1^2}{2} + \frac{\gamma}{\gamma - 1}\frac{p_1}{\rho_1} = \frac{u_2^2}{2} + \frac{\gamma}{\gamma - 1}\frac{p_2}{\rho_2},$$

Piston-driven shock wave

[1] X. Zhang et al., Nucl. Fusion 64, 096005 (2024).

Applications of Hybrid-PIC code “Ascent-Hybrid” in ICF

◆ **Ascent-Hybrid:** successfully used to study of shock wave, hydrodynamic instabilities, and implosions in ICF

counter-propagating plasma shocks in the hohlraum

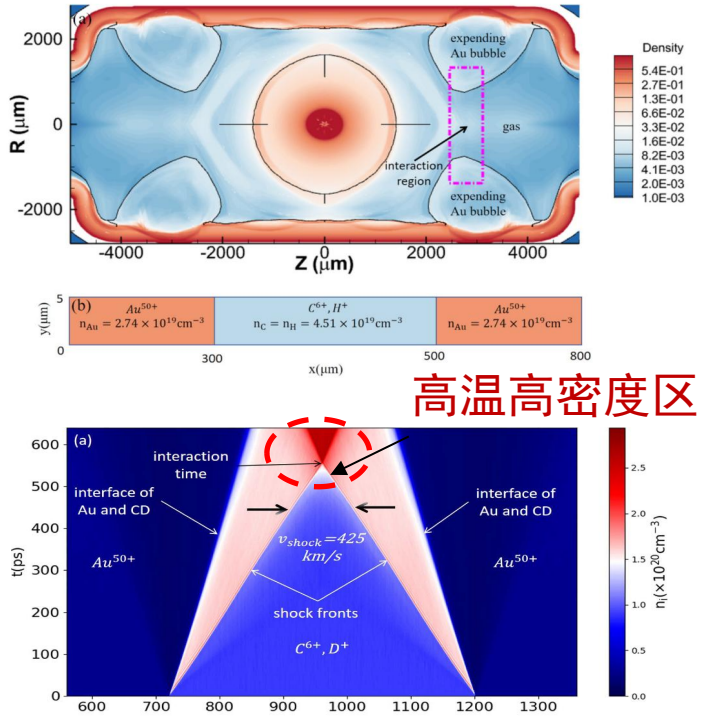

[1] Nuclear Fusion, 64, 096005 (2024)
[2] PPCF 67, 115001 (2025)
[3] PPCF 67, 055048 (2025)

shock interaction with highly nonuniform plasmas

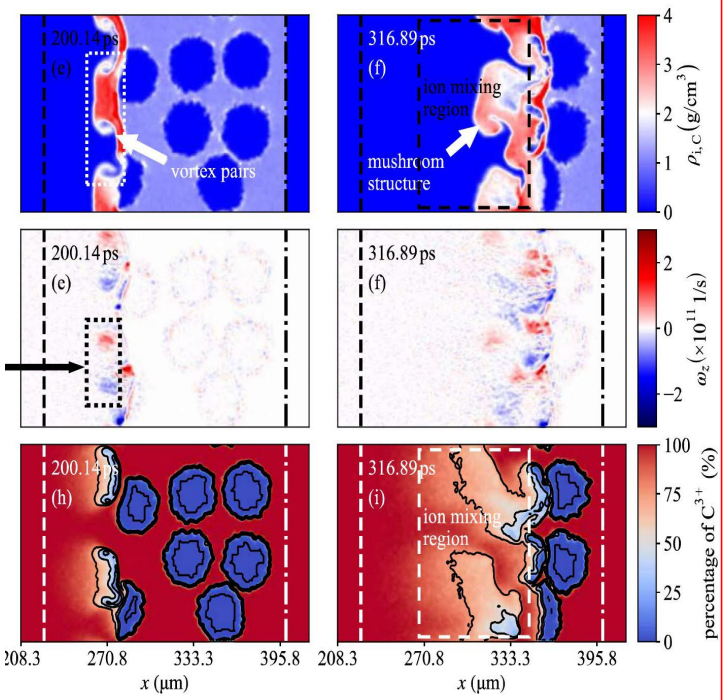

[4] Nucl. Fusion 65, 066009 (2025)
[5] NJP, 26, 063039 (2024)
[6] POP 31, 052105 (2024)

material mixing in an indirect-drive ICF implosion

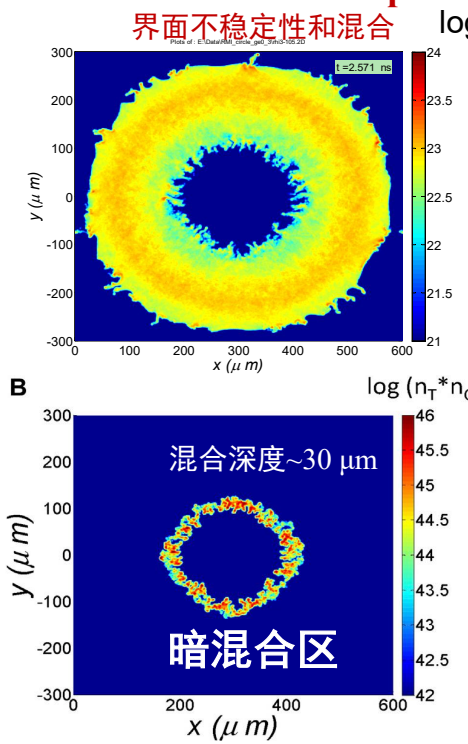

[7] New Journal of Phys., 23, 053010 (2021)
[8] Frontiers in Physics 11, 1140383 (2023)
[9] Phys. Plasmas 32, 082111 (2025)

Outline

- Development of Hybrid fluid-PIC code for ICF
- Characteristics of shock waves in HED plasmas
- Characteristics of hydrodynamic instabilities in HDP plasmas

Shock wave overtaking in HED plasma: ICF target pellet implosion

- In ICF implosion, increasing a strong shock strength does not lead to appreciable increase of the compression.
- Fast and nearly isentropic compression can be achieved by superimposing a sequence of shock waves.
- Therefore, where the shock waves converge is the key issue affecting the implosion performance of ICF.

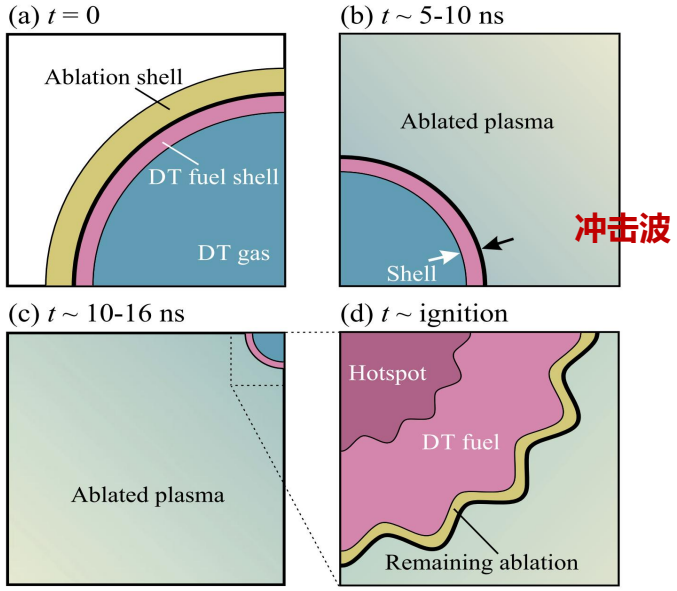

ICF内爆

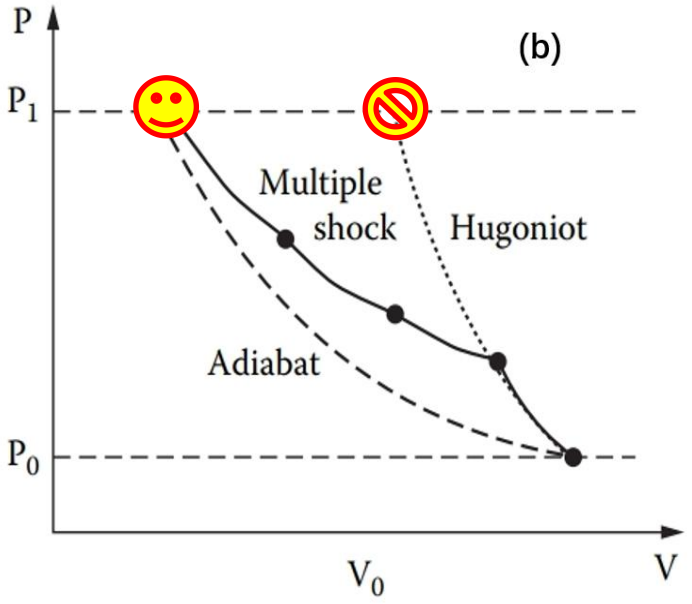

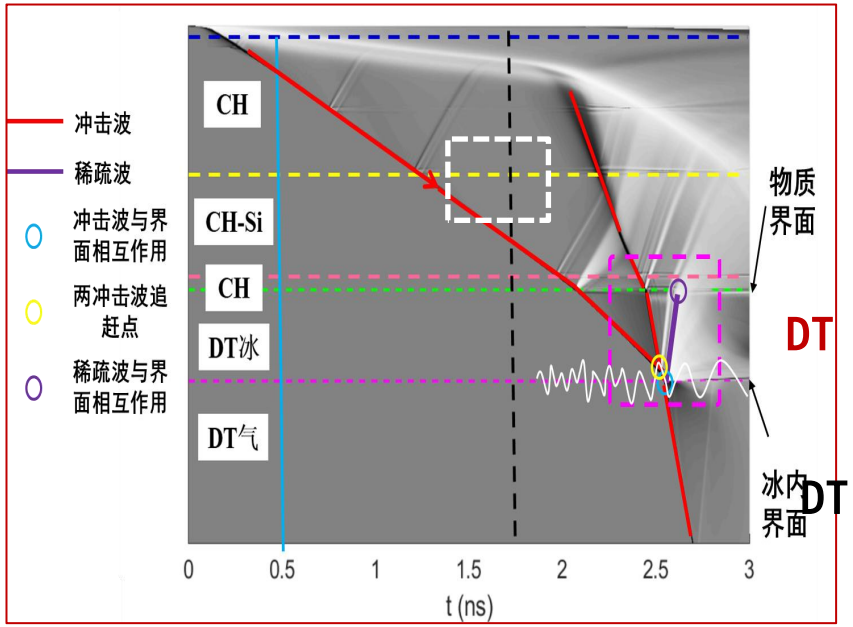

- Question: To ensure implosion performance, the shock waves should converge near the DT **ice-gas** interface. However, some experiment results deviates too much from the RH simulation prediction. Why?

Shock wave converging in HED plasma: ICF target pellet implosion

- **1. Shock wave converging in the solid density region (DT ice): (shocks: v_{s1}~300km/s, v_{s2}~824km/s, M~2.15)**
- When shocks propagate in DT ice region, the kinetic effects are weak, the material pressure after the convergence of two shock waves matches the fluid simulation well.

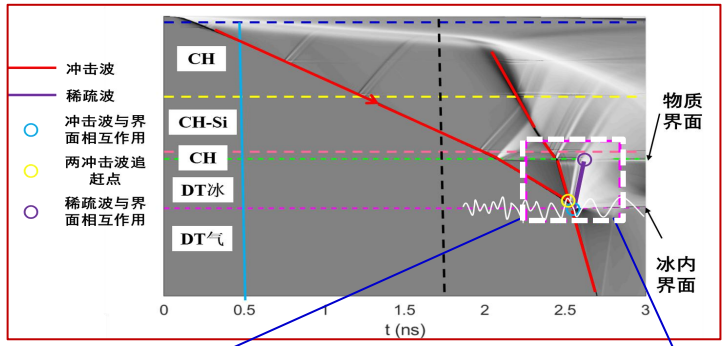

DT ice

DT gas

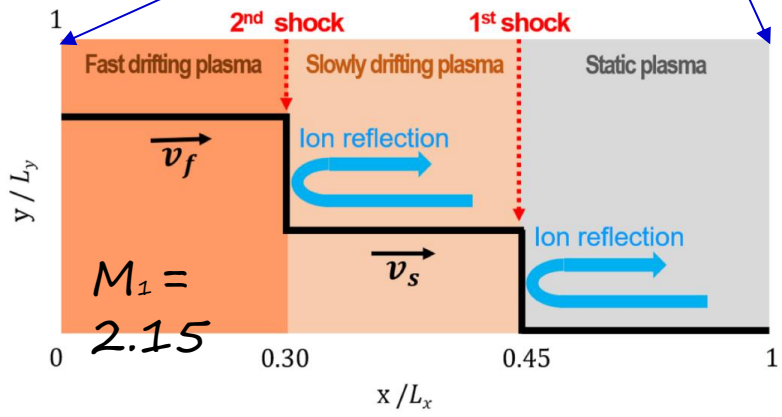

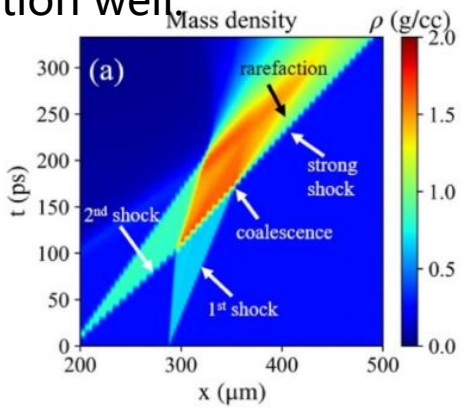

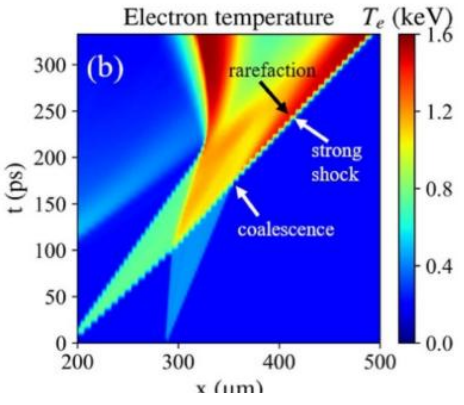

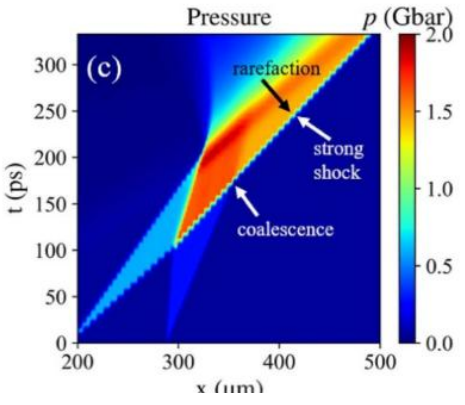

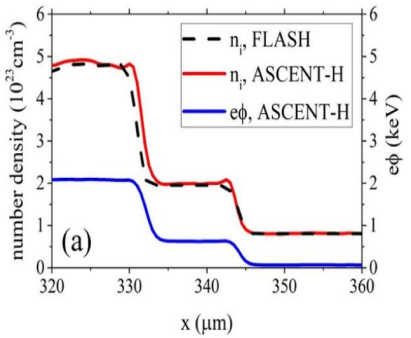

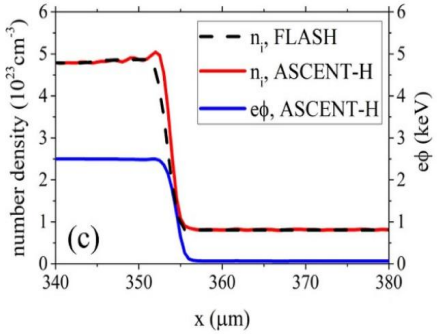

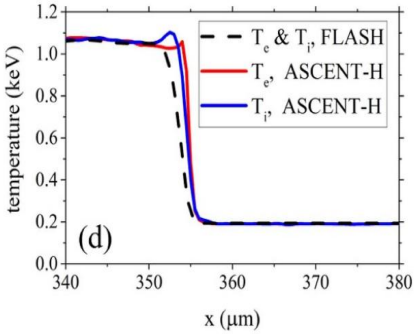

ρ_{DT} = 250mg/cc

n_{merger}/n_{u1} = 5.9

P_{Hybrid}/P_{Flash} = 98%

Shock wave converging in HED plasma: ICF target pellet implosion

- **2. Shock wave converging in the low-density region (DT gas): (shocks: v_{s1}~300km/s, v_{s2}~824km/s, M~2.0)**
- During the propagation of shock wave in low-density DT gas region, it drives high-energy ions (>10keV) to preheat the wavefront region, reducing the material pressure significantly to 77% of the estimated value.

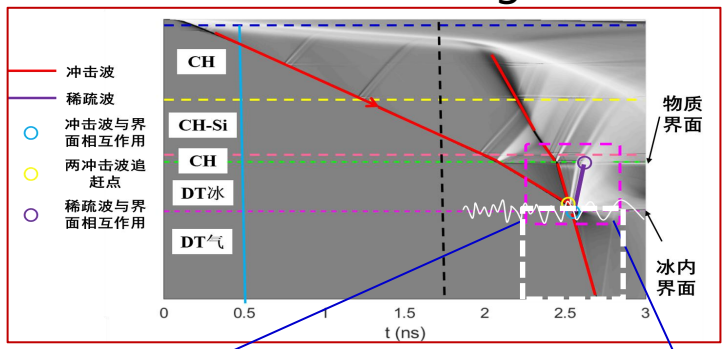

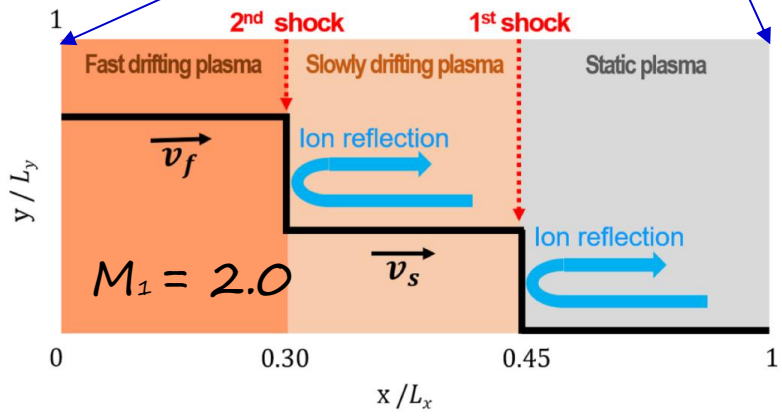

DT ice

DT gas

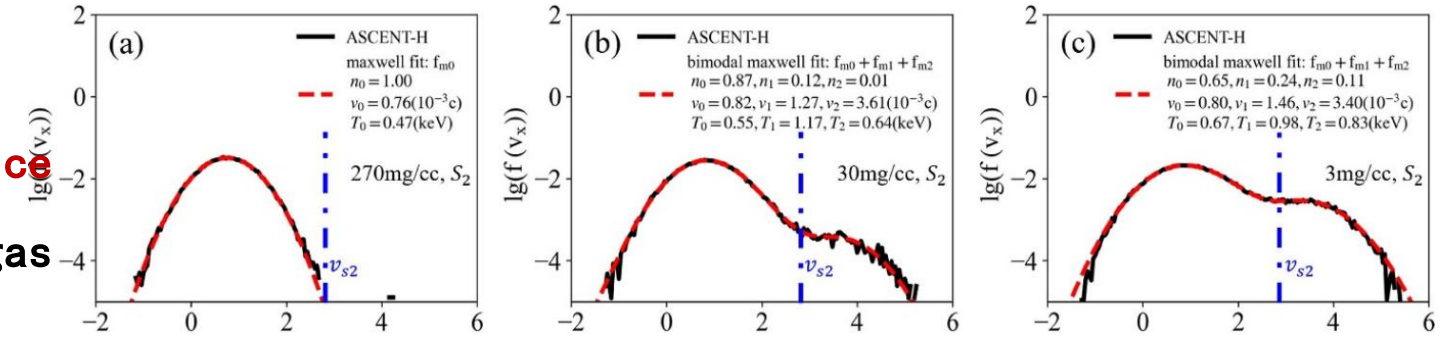

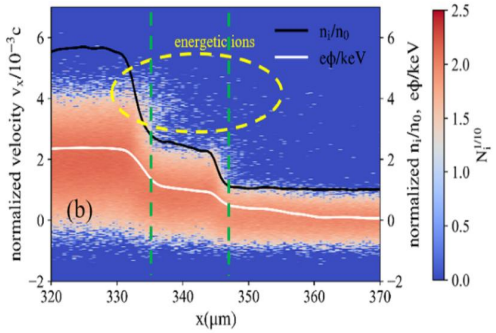

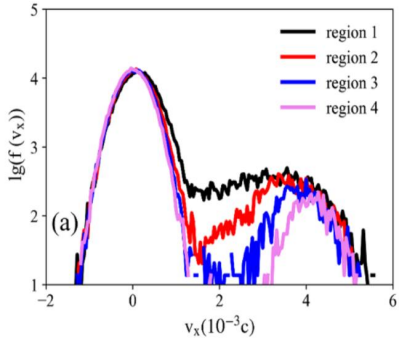

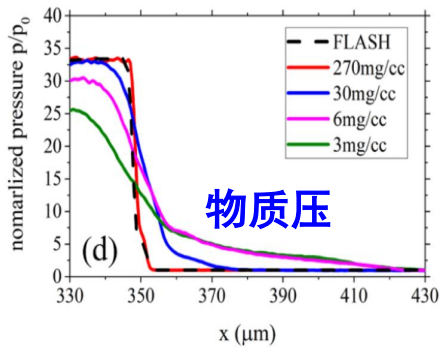

$\rho_{DT} = 3mg/cc$

$n_{merger}/n_{u1} = 5.5$

$P_{Hybrid}/P_{Flash} = 77\%$

Shock wave converging in HED plasma: ICF target pellet implosion

- Ascent-Hybrid simulations explained why the hot spot pressure and implosion performance are much lower than RH prediction in some the ICF shots on the Shenguang laser facility.
- To ensure implosion performance, the shock waves should converge near the DT ice-gas interface on one side of ice.

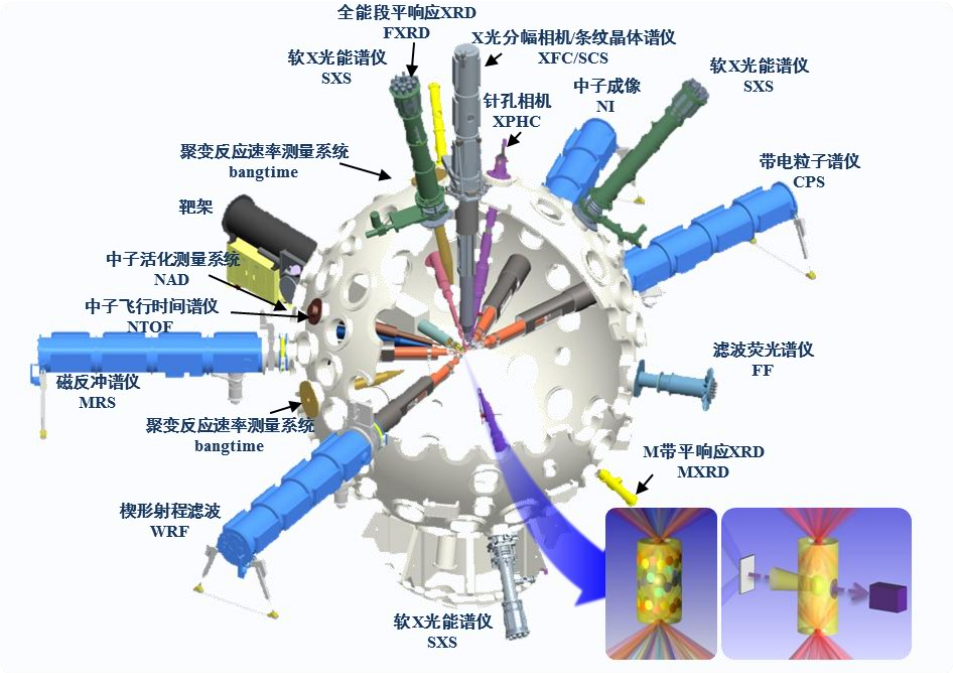

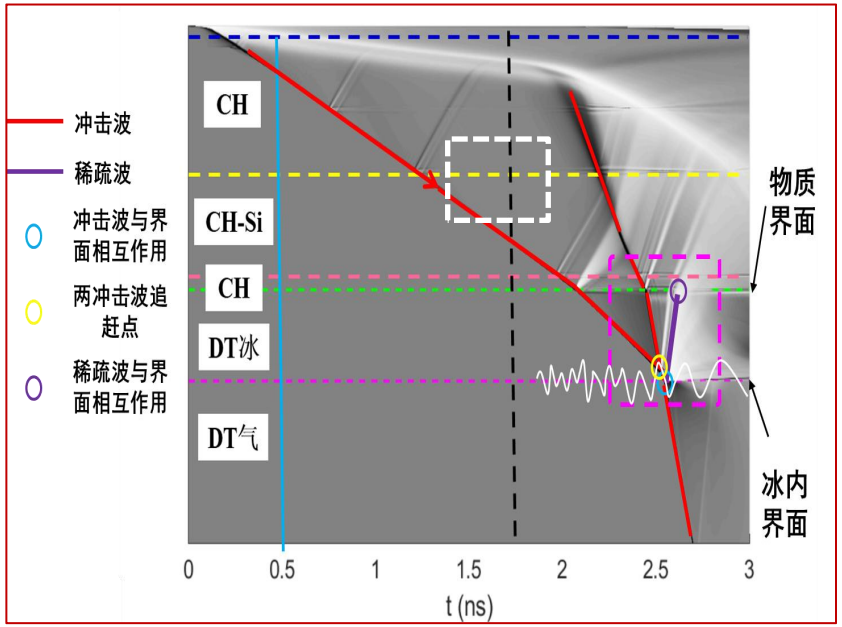

DT ICE

DT gas

[1] E.H. Zhang et al, Plasmas Phys. Controlled Fusion 67, 055048 (2025)
[2] Y.P. Xu et al., Phys. Plasmas 31, 052105 (2024)

Why are multiple shock waves converging so differently in DT ice and gas?

The change of shock wave structure is significant: from collision to collisionless dominant

In collisionless-dominant region, the energetic ions can be reflected by the electric field at the shock front, usually have a velocity $v_d \sim 2v_s$. The ion kinetic effects play important roles in strong shocks.

- **Collision-dominated region:**

  The ion kinetic effect is weak, and the ion temperatures are not separated

- **Transition region:**

  Ion temperatures detachment at the wavefront

- **Collisionless-dominant region:**

  non-equilibrium, and significant kinetic characteristics

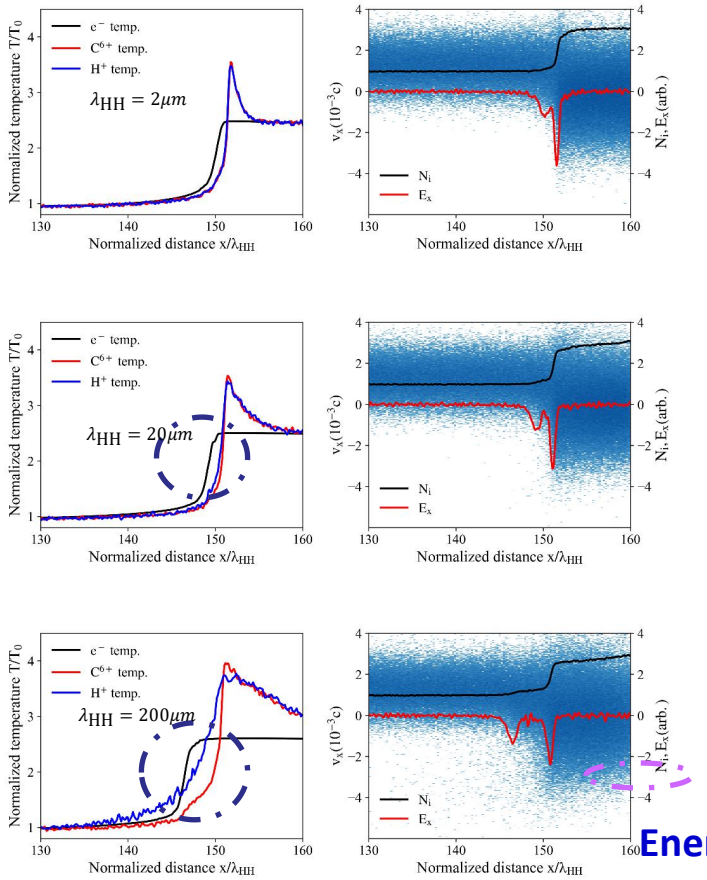

$10^{23}cm^{-3}$

$10^{22}cm^{-3}$

$10^{21}cm^{-3}$

density n_e

[2] E. Zhang et al., Influence of the electron thermal conduction and ion kinetic effects on the structure of collisional plasma shocks, Phys. Plasmas 29, 082110 (2022)

Outline

- Development of Hybrid fluid-PIC code for ICF
- Characteristics of shock waves in HED plasmas
- Characteristics of hydrodynamic instabilities in HDP plasmas

Hydrodynamic instabilities and ion mixing present significant challenges in ICF

During the ICF implosion, the target imperfection will be catastrophic amplified under extreme conditions, affecting the success of ignition

Hydrodynamic instability of target imperfection amplification

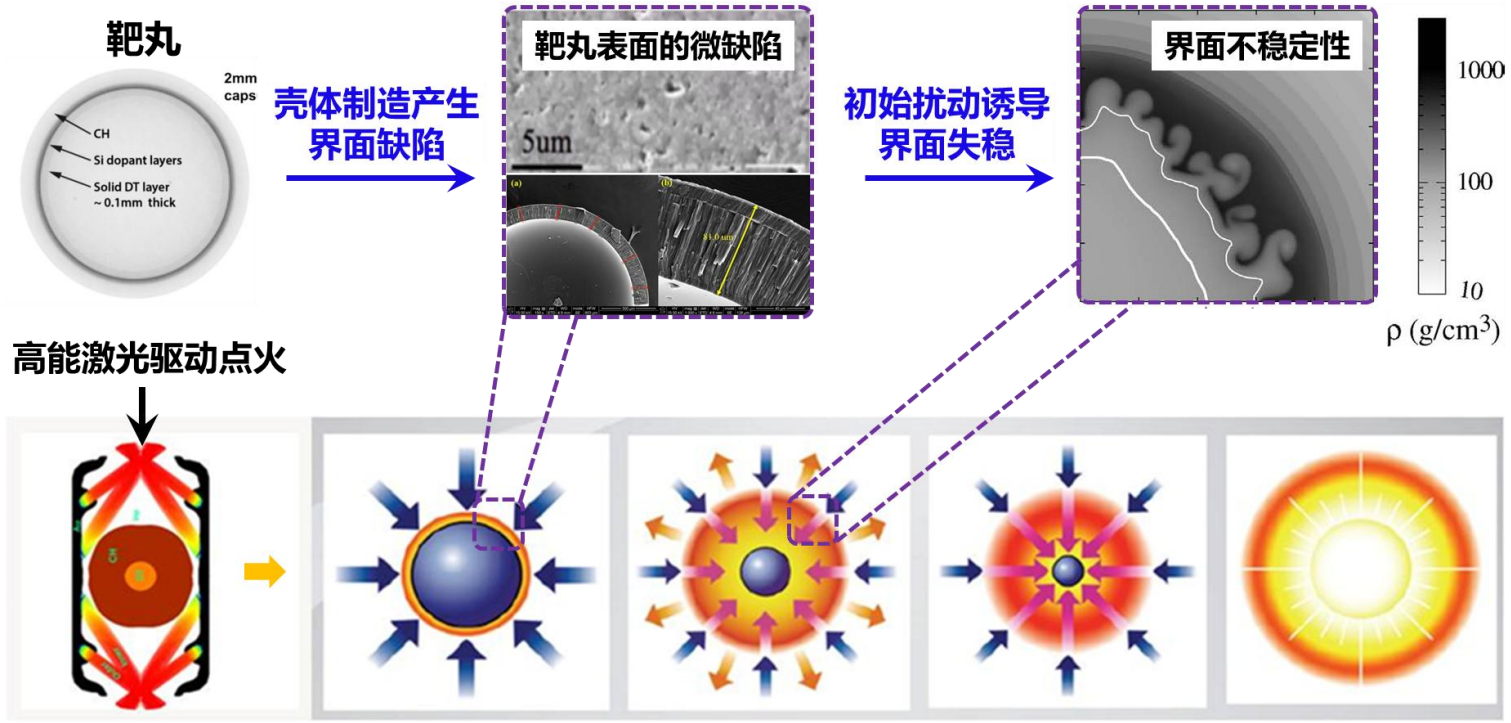

Instability exponential growth affects ignition success

$$\eta \sim \eta_0 e^{\gamma(k)t}$$

- Defect size $\Rightarrow \eta_0$
- Number of defects $\Rightarrow k$

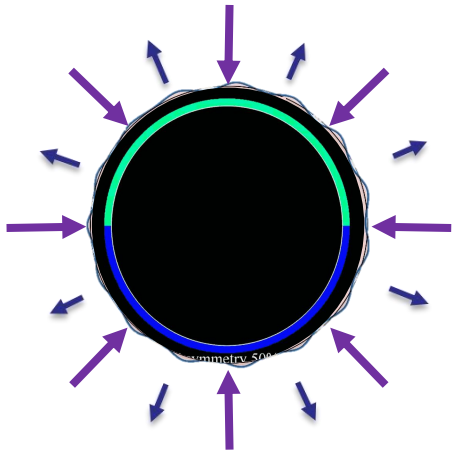

Hydrodynamic instabilities and ion mixing present significant challenges in ICF

◆ICF: With the development of HI, **ion mixing** occurs at the ablator-fuel interface, which affects the conditions and margins of fusion ignition, as well as the rate and depth of fusion combustion

◆NIF experiments have shown that the fusion yield drops quickly even with < 0.5 μg ablator mixing into the fuel

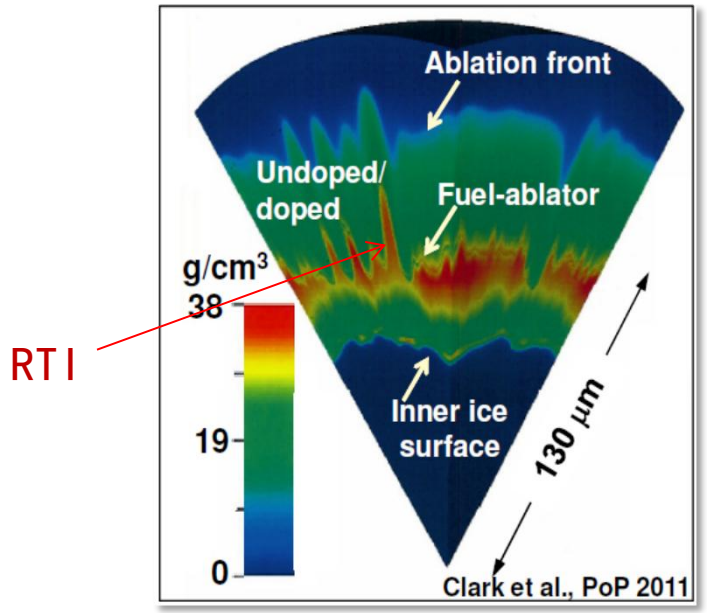

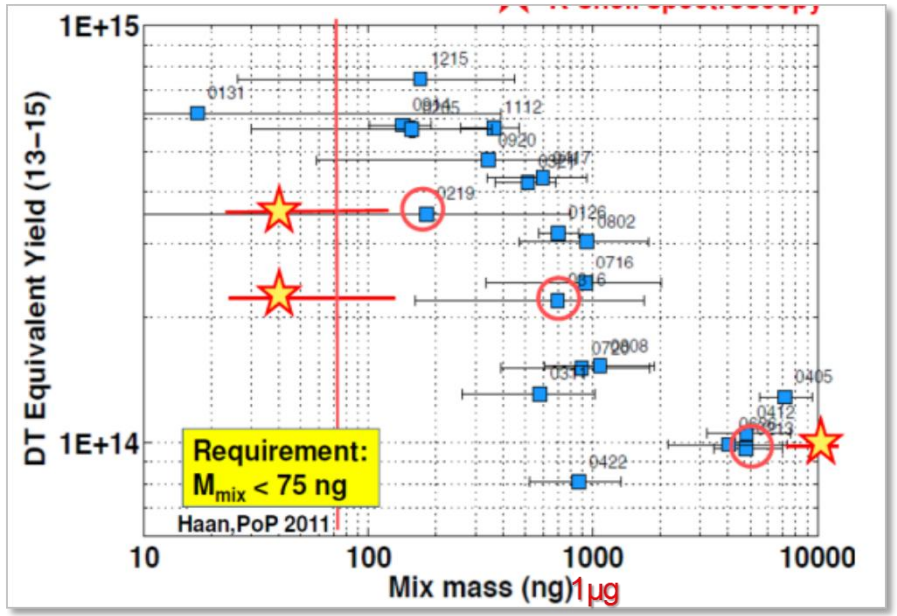

Ma et al., PRL, 2013

Bayesian analysis

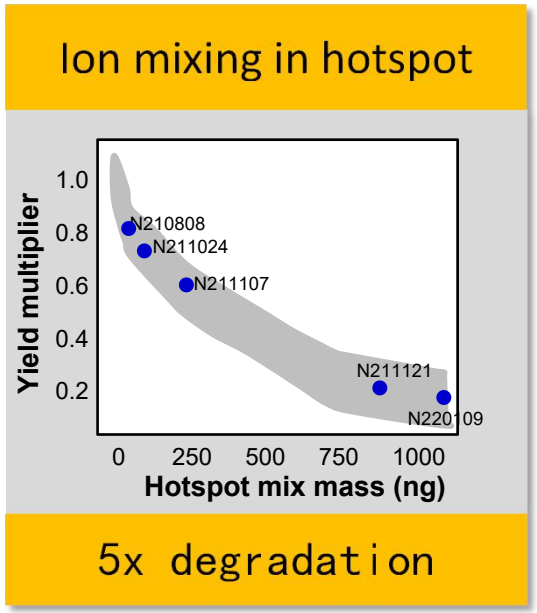

L.Divol et al., APS, 2022

◆How to study the ion mixing due to Hydrodynamic instability in ICF implosion process？ （**Problem 2**）

Hybrid fluid-PIC simulation of Richtmyer–Meshkov instability

Ascent-Hybrid is used to study the Effect of kinetic effects on the evolution of RMI and mix

Sinusoid Perturbation: λ=4μm, a_0=1, 2 μm

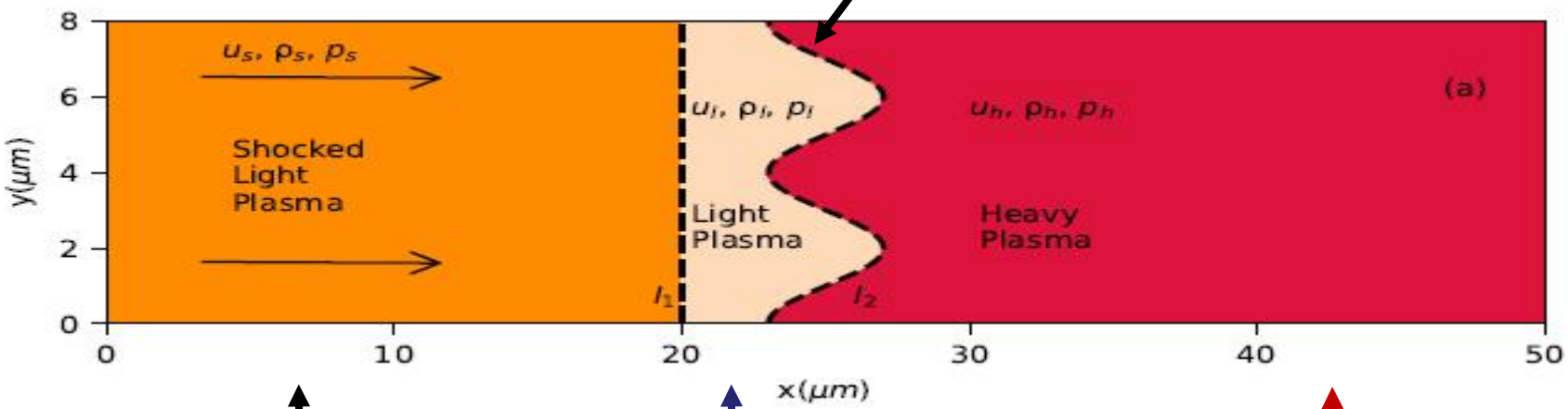

Moving plasma（H+）
u_d=0.01c
m_i=1836m_e
Z=1，A=1
n_e=4.9×10^{23} cm^{-3}
T_e=T_i=0.1keV

Light plasma（H+）
u_d=0
m_i=1836m_e
Z=1，A=1
n_e=4.9×10^{23} cm^{-3}
T_e=T_i=0.1keV

Heavy plasma（C^+）
u_d=0
m_i=22032m_e
Z=1，A=12
n_e=4.9×10^{23} cm^{-3}
T_e=T_i=0.1keV

The hybrid-PIC simulations can capture the interfacial mix during the evolution of RMI and its effect

With the development of RMI, low-Z ions mix into the high-Z plasma, affect the viscosity and transport coefficient, and further affect the evolution of instability

Evolution of mass density (g/cc)

t

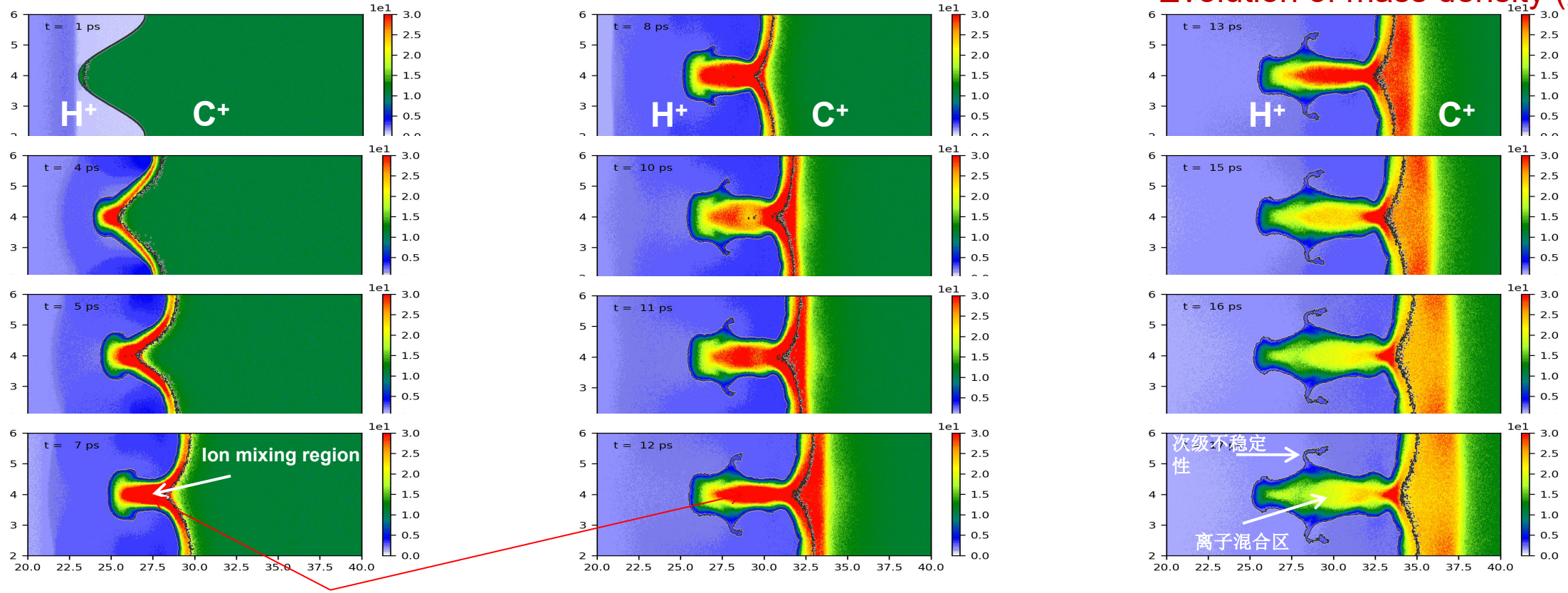

The region between two black lines is C/H mixing region, which can not be captured by fluid simulation.

Solve the difficulty of fluid code not being able to consider EM fields

- EM fields affect electron heat conduction ➔ temperature(pressure) gradient ➔ affect the evolution of RMI

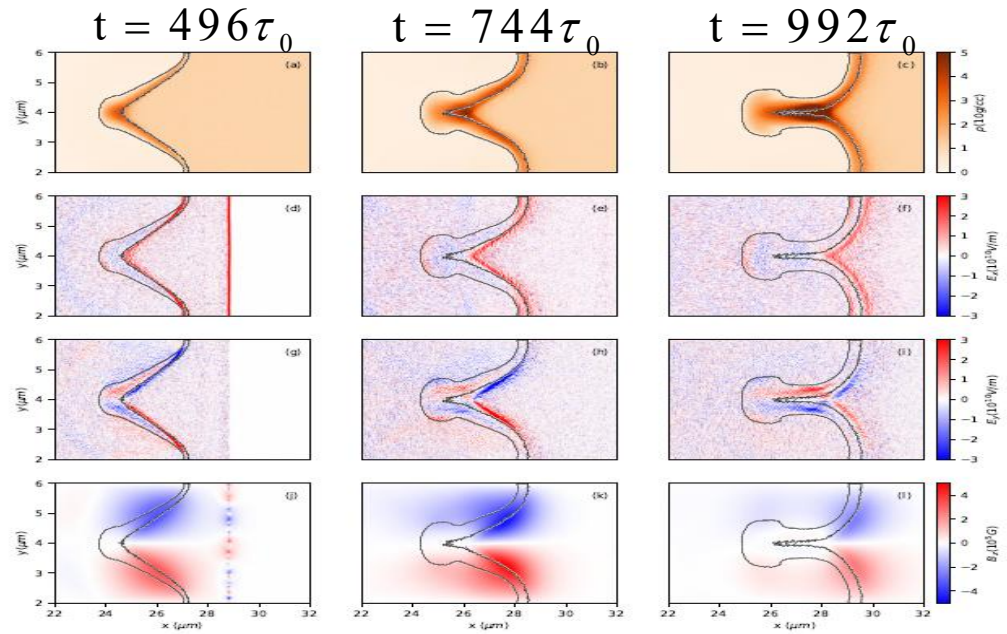

E-field $\mathbf{E} = \left(\eta_{\|}\mathbf{J}_{\|} + \eta_{\perp}\mathbf{J}_{\perp}\right) - \mathbf{V}\times\mathbf{B}/c - \frac{1}{en_e}\left(\nabla p_e - \mathbf{R} - \mathbf{J}\times\mathbf{B}/c + \nabla q_v\right)$

B-field $\frac{\partial \mathbf{B}}{\partial t} = \nabla\times(\mathbf{V}\times\mathbf{B}) - \nabla\times\left(\frac{\mathbf{J}}{en_e}\times\mathbf{B}\right) + c\nabla\times\left(\frac{\nabla p_e}{en_e}\right) - c\nabla\times\left(\frac{\mathbf{R}_T}{en_e}\right) - c\nabla\times\left(\eta_{\|}\mathbf{J}_{\|} + \eta_{\perp}\mathbf{J}_{\perp}\right)$

Self-generated E-feild: $E_{max} \sim 4\times10^{10}\,V/m$

Self-generated B-field: $B_{max} \sim$ 70-100 Telsa

Vorticity $\frac{\partial \boldsymbol{\omega}_\alpha}{\partial t} - \nabla\times(\nabla\times\boldsymbol{\omega}_\alpha) - \frac{1}{\rho_\alpha^2}(\nabla\rho_\alpha\times\nabla p_\alpha) = \nabla\times\left(\frac{q_\alpha}{d_L m_\alpha}(c\mathbf{E} + \mathbf{u}_\alpha\times\mathbf{B})\right)$

Baroclinic term: affect heat conduction

[1] X.X. Yan et al., New Journal of Phys., 23, 053010 (2021)

[2] F.Q. Meng et al., New Journal of Physics, 26 063039 (2024)

The development of RMI means that low-Z ions mix into the high-Z plasma, forming an ion mixing region.

- Ion mixing brings changes in viscosity and transport coefficient, which then affects the evolution of RMI
- **How to study it quantitatively?**

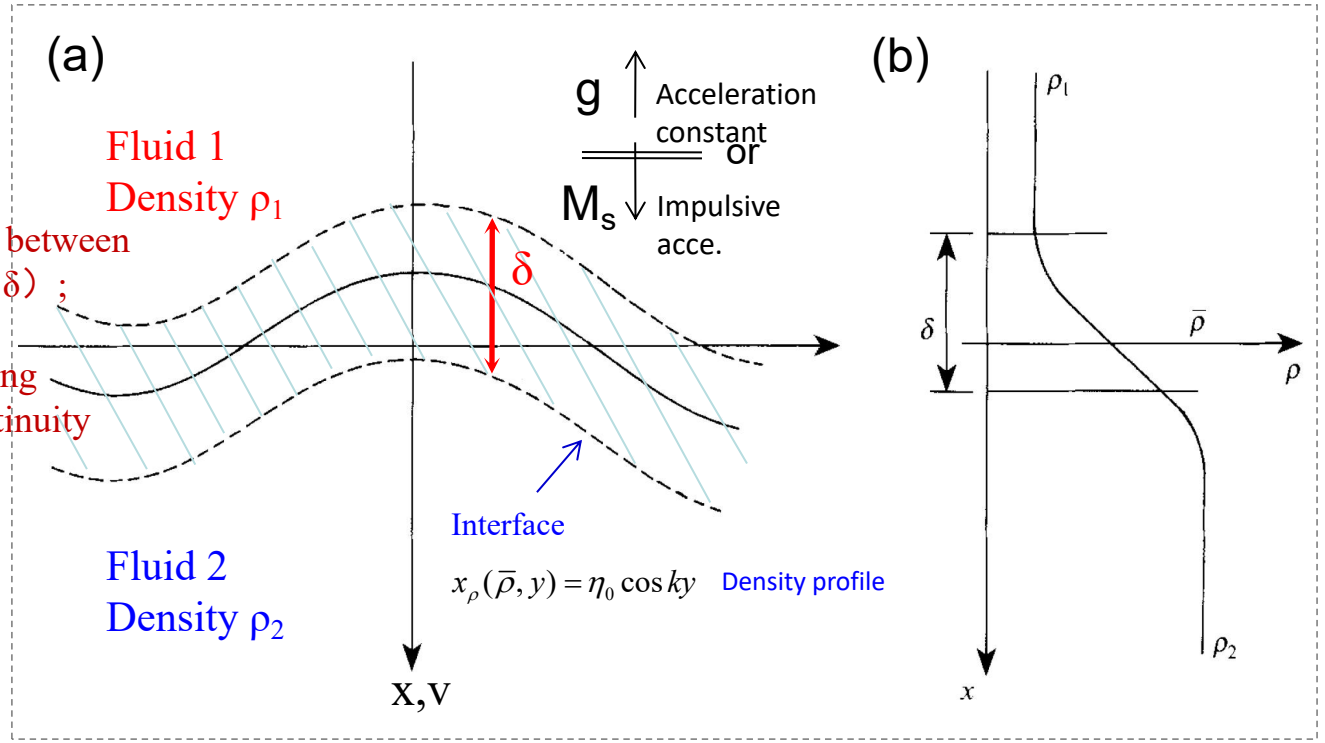

- Braginskii kinematic viscosity

$$\nu_{avg} = 3.3\times10^{-5}\frac{\sqrt{A}T^{5/2}}{Z_{eff}^4\rho\ln\Lambda}$$

$$Z_{eff} = x_1Z_1 + x_2Z_2$$

- RMI growth rate

$$\dot{\eta}_{Mikaelian} = \frac{k\eta_0 A u_c}{\psi(k,D,t)}\exp\left[-2k^2\nu_{avg}t\right]$$

[1] M. Brouillette et tl., JFM 1994

After considering time-varying viscosity coefficients and modified diffusion widths, the simulation results closely match the theoretical values

The eigenvalue eq. for the perturbation velocity of RMI:

$$\frac{\mathrm{d}}{dx}\left(\rho\frac{du}{dx}\right)=uk^2\left(\rho-\frac{\psi}{Ak}\frac{d\rho}{dx}\right)$$

Ψ is the growth reduction factor. The density profile of the mixing layer:

$$\rho(x)=\bar{\rho}\left[1+\bar{A}erf\left(\frac{x}{\delta}\right)\right]$$

δ is the thickness of the mixing layer. The RMI growth rate is given by Mikaelian

$$\dot{\eta}_{Mikaelian}=\frac{k\eta_0 Au_c}{\psi(k,D,t)}\exp\left[-2k^2v_{avg}t\right]$$

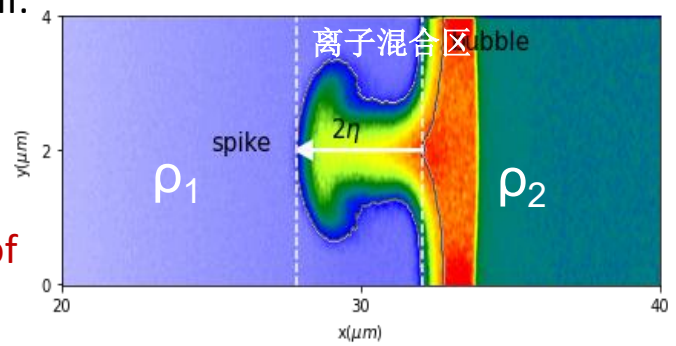

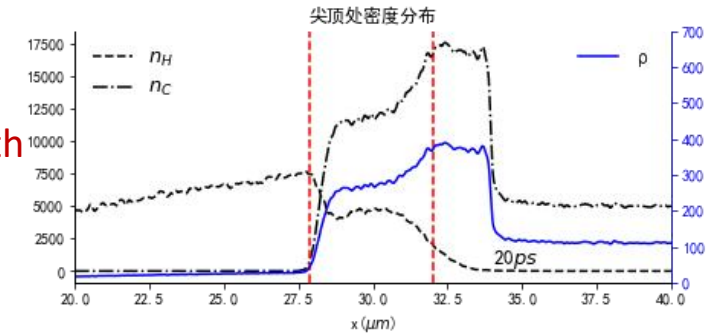

Atwood ~ 0.5

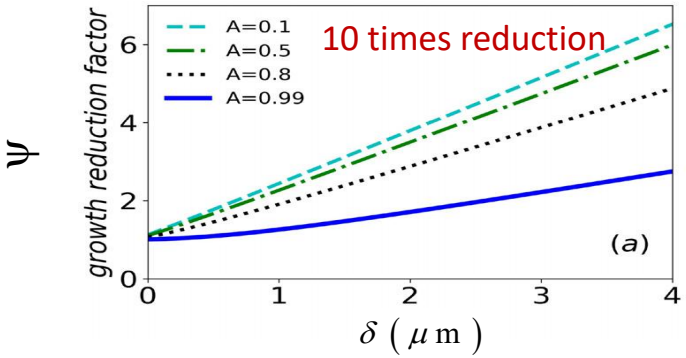

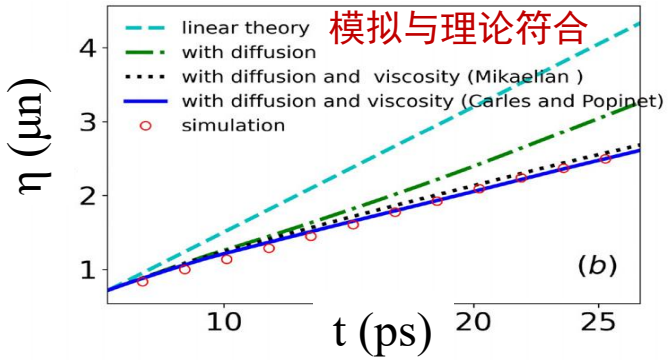

The growth reduction factor Ψ reaches as high as 10 as the thickness δ~8 μm .
The simulation results are consistent with the theoretical estimate considering the ion diffusion and mixing.

To elucidate the influence of viscosity on the evolution of RMI with greater clarity, the Coulomb logarithm was artificially adjusted

In the case of (1/5)lnΛ, an increase in viscosity results in a notable enhancement of ion diffusion and mixing, which in turn leads to a substantial reduction in RMI amplitude

In the case of 5lnΛ, the viscosity decreases significantly, RMI development becomes more pronounced, and the spike structures are well-defined, potentially leading to the emergence of secondary instabilities.

- Braginskii kinematic viscosity

$$\nu_{avg} = 3.3\times10^{-5}\frac{\sqrt{A}T^{5/2}}{Z^4\rho\ln\Lambda}$$

- RMI growth rate

$$\dot{\eta}_{Mikaelian} = \frac{k\eta_0 A u_c}{\psi(k,D,t)}\exp\left[-2k^2\nu_{avg}t\right]$$

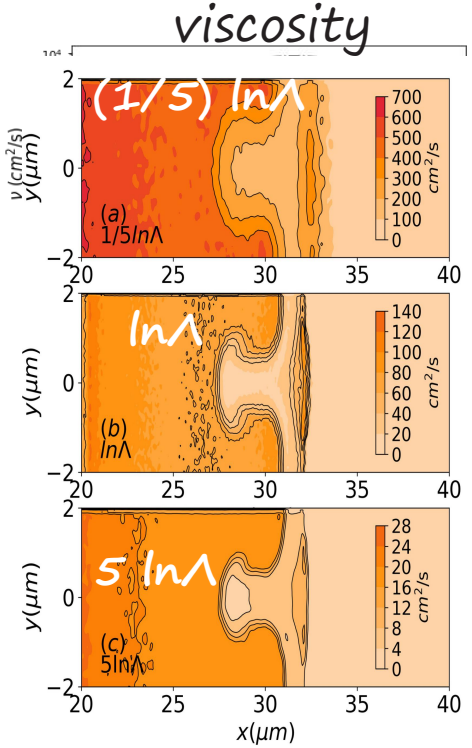

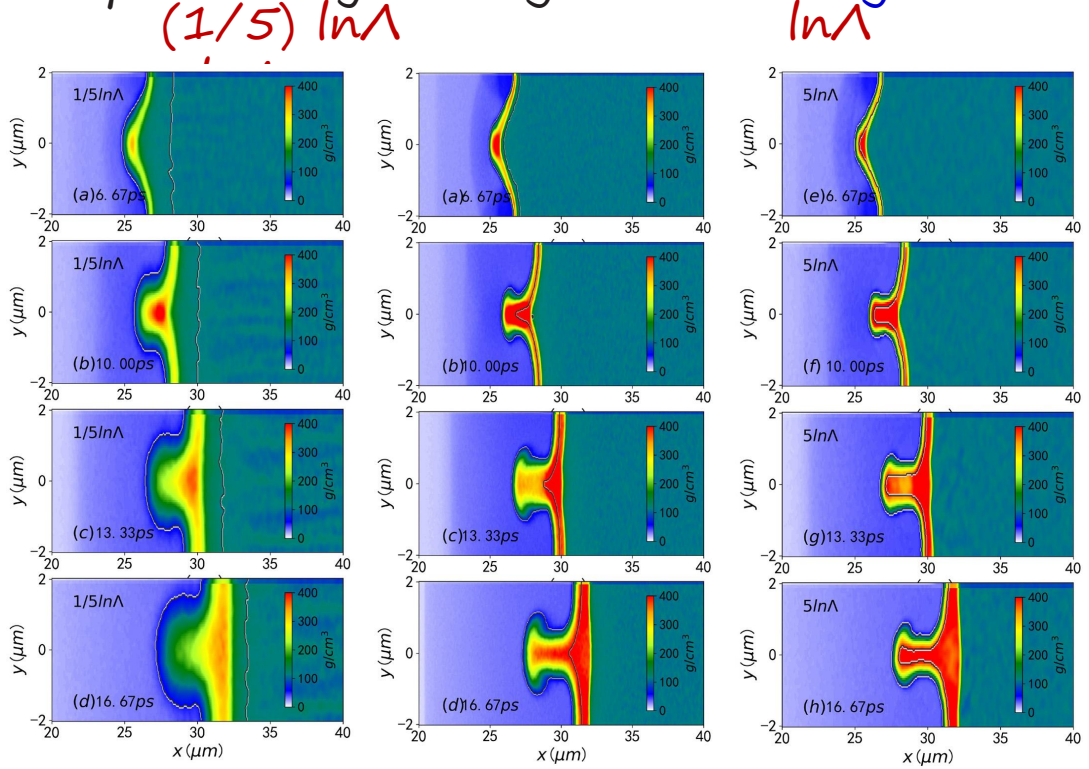

[1] H.X. Huang et al.， Physics of Plasmas (2025)

[2] Z. H. Lin et al., Phys. Plasmas 32, 082111 (2025)

How do ion diffusion and mixing affect the RMI structure and evolution during a phase inversion?

When the shock wave passes through the heavy/light interface, with inversion of the RMI, the RMI rapidly develops into a non-linear phase. This causes low-Z ions to quickly mix with high-Z ions, which affects the viscosity and transport coefficients.

The mixing layer suppresses the growth of RMI amplitude and inhibits the formation of nonlinear structures through the time-varying Atwood number and self-consistent ionic kinematic viscosity $\nu(t)$ compared with the hydrodynamic simulations

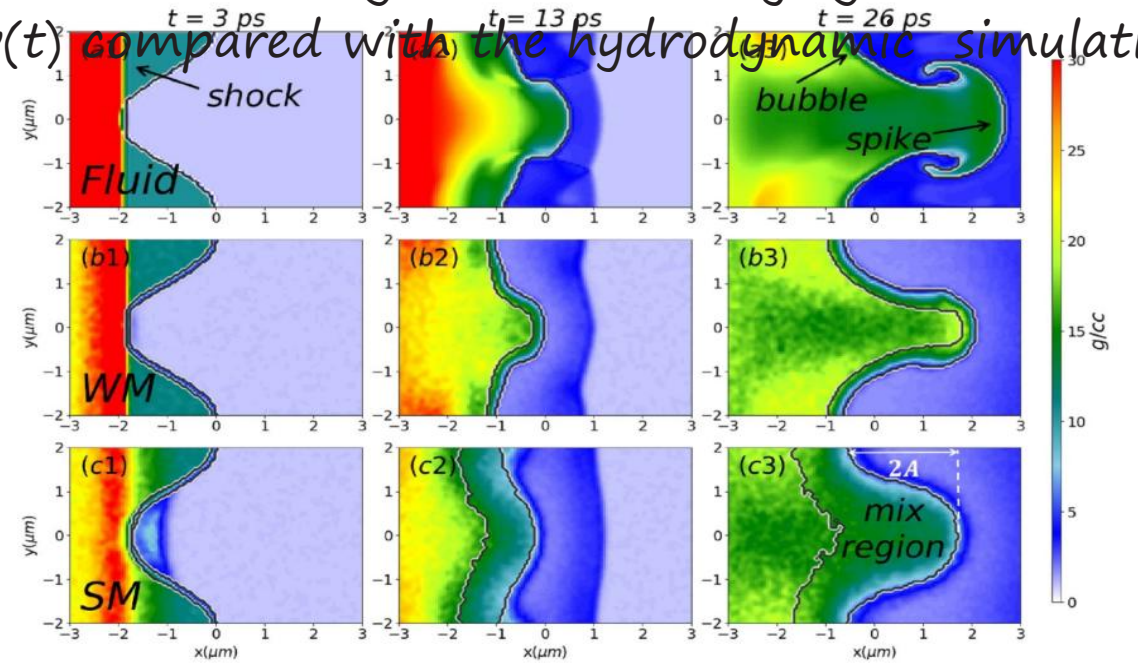

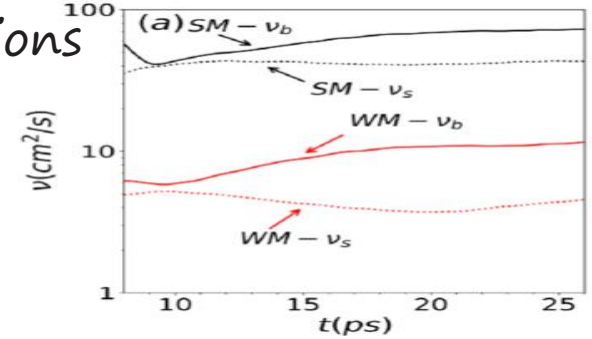

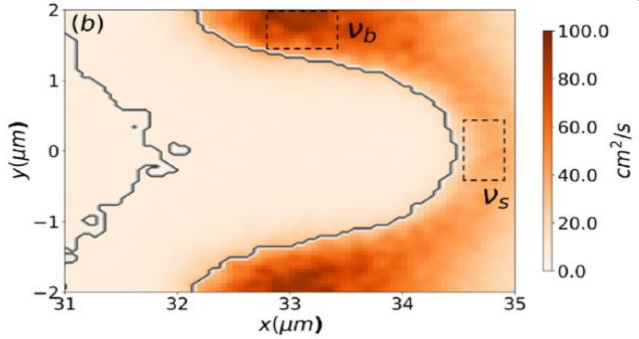

- Dimonte and Ramaprabhu (DR) model

$$\dot{A}_{b,s}^{NL} = \frac{1 + (1 \pm |A_T|)\, k\delta V t}{\left[1 + C_{b,s} k\delta V t + (1 \pm |A_T|)\, F_{b,s} (k\delta V t)^2\right]} \delta V$$

$$C_{b,s} = \frac{4.5 \pm |A_T| + (2 \pm A_T)\, C_c k a_0}{4}$$

$$F_{b,s} = 1 \mp A_T.$$

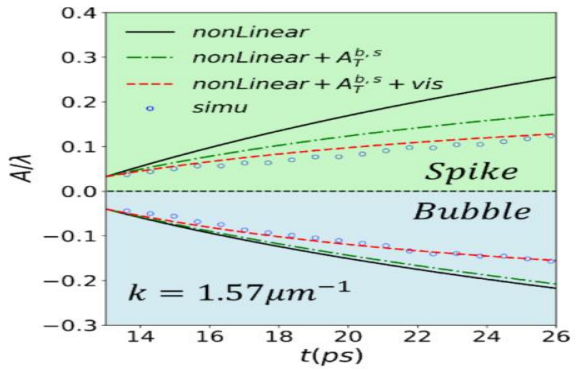

[1] Mingjun Chen et al.， Nuclear Fusion, 65, 066009 (2025)

[2] F.Q. Meng et al. , PPCF 67, 085014 (2025)

Experimental verification: Richtmyer–Meshkov instability

We observed the evolution of RMI by proton and x-ray radiography. The experiments are reproduced by RH simulation.

Inversion from proton radiography shows magnetic B~5 Telsa; Ion mixing process will be next aim.

(a) Schematic

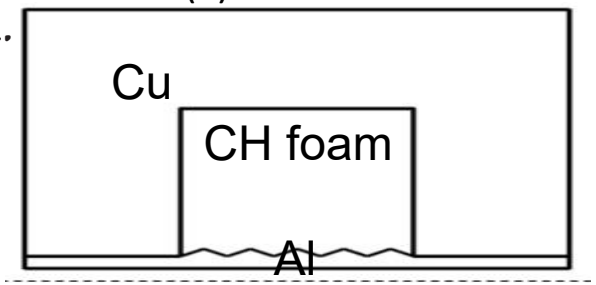

(b) Target

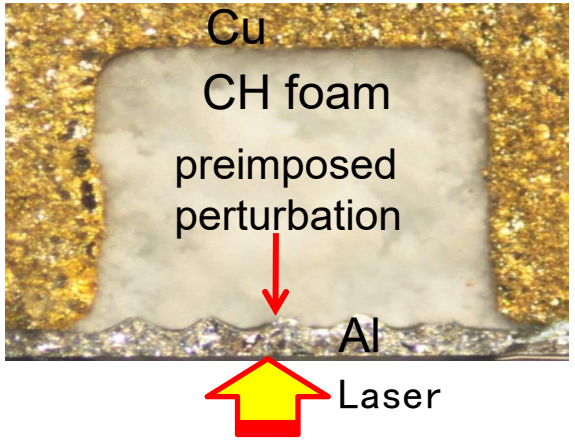

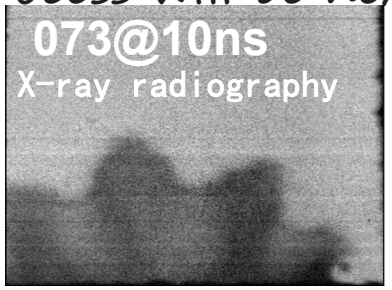

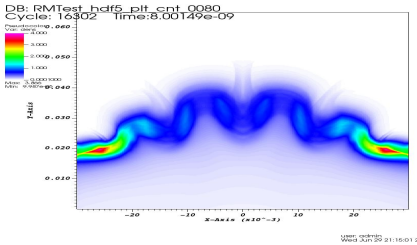

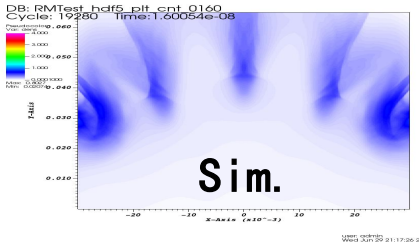

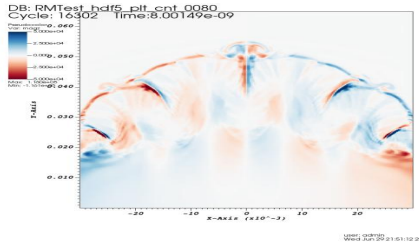

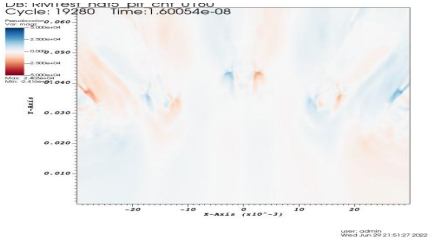

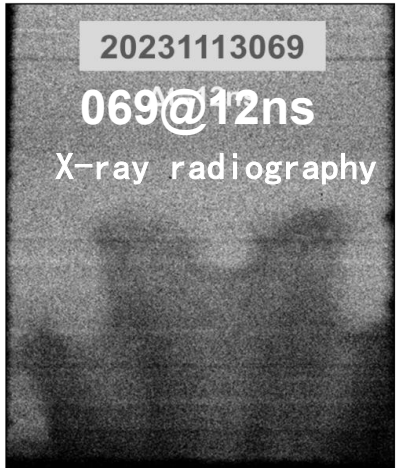

[1] P.L. Yao et al.， prepare to submit

Summary

•We have developed a hybrid fluid-PIC code Ascent-H to model the shock wave and hydrodynamic instabilities.

•Hybrid fluid-PIC simulations aimed at a better understanding of the effect of ion diffusion and viscosity on the evolution of Richtmyer–Meshkov instability (RMI) under high temperature and high density conditions are described.

Thanks for your attention!

Application II: Evolution of Rayleigh-Taylor instability

2.1 Role of kinetic effects in evolution of the Rayleigh-Taylor instability

- With the increase of Knudsen number (kn=λ_{ii}/L), the secondary instabilities (KHI) are suppressed significantly by the viscosity.

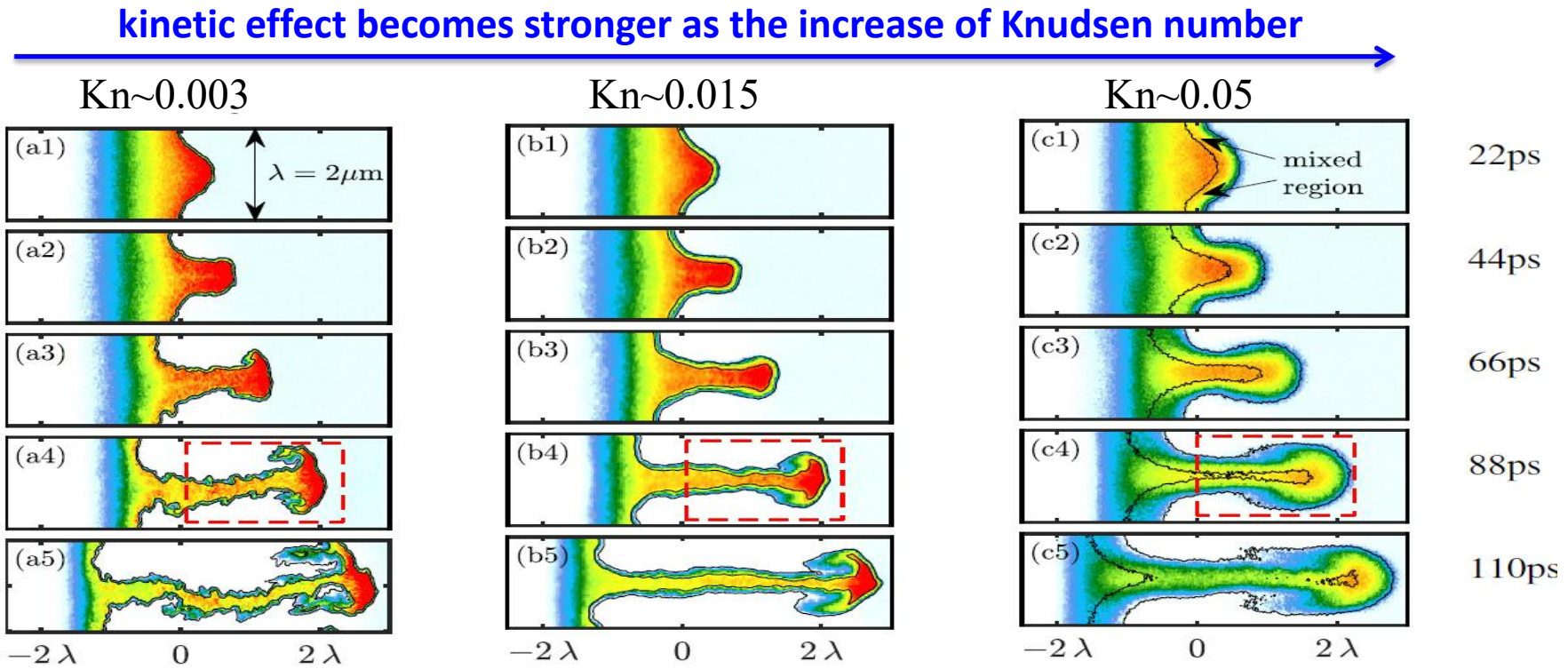

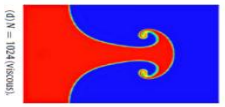

Gravity：g=2.4×10^{17}cm/s^2； Atwood number：0.85； n_e=9.2e23 cm^{-3}

λ_{ii}=3.6μm, 36μm, 360 μm

$T_e = T_i = 0.2keV$, $a_0/\lambda \sim 0.83$

[1] P.L. Yao, H.B. Cai* **et al., Nuclear Fusion**, under Review

How the capsule imperfections affect the ICF implosion performance?

- **We simply the capsule imperfection problem into a shock-bubble interaction in multi-species plasmas**
- Significant shock-induced ion mixing, driven by both the shock-accelerated fast ions (one of the ion kinetic effects) and the plasma diffusion, increased the viscosity. This viscosity persistently dissipates the vorticity.

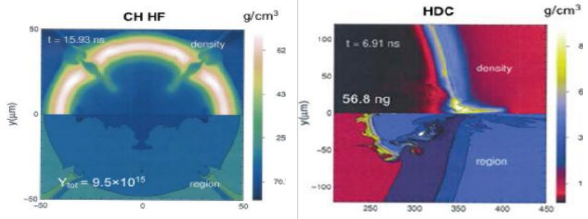

支撑膜 Filled pipe

ICF靶丸界面失稳种子

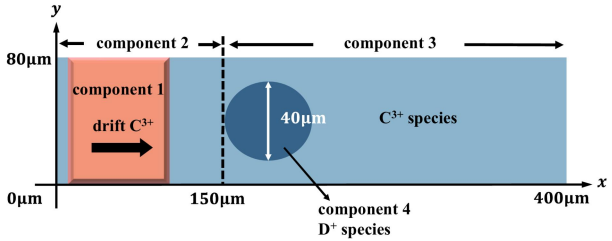

环量 $\Gamma = \int dt \iint_S dxdy \left[-\boldsymbol{\omega} \cdot (\nabla \cdot \mathbf{V}) + \frac{\nabla\rho \times \nabla p}{\rho^2} + \nu\nabla^2\boldsymbol{\omega} - \frac{\nu}{\rho}(\nabla\rho \times \nabla^2\mathbf{V}) \right]_z$

Γ_{dila} Γ_{baro} Γ_{visc}

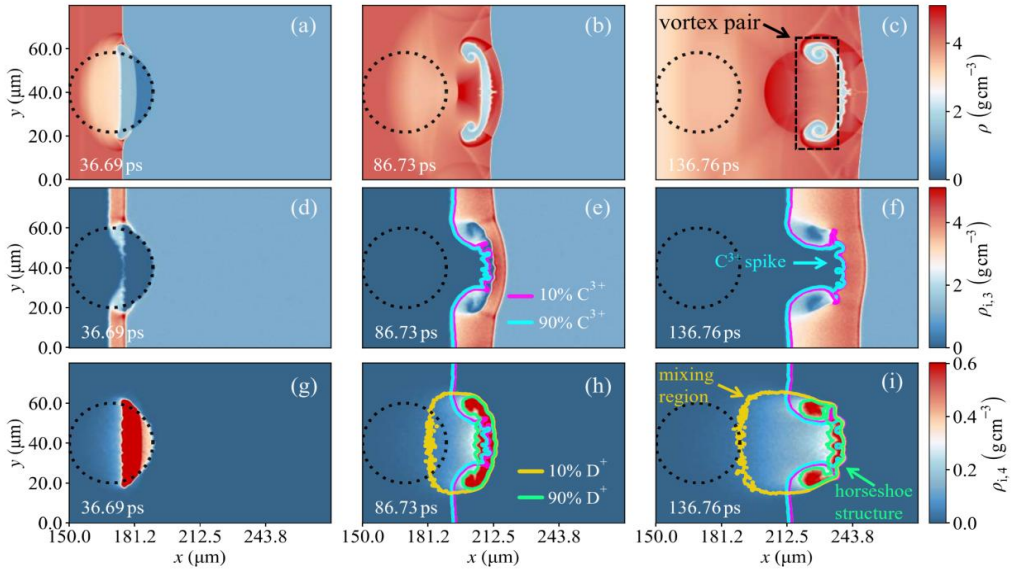

RH simulation

Hybrid simulation

C^{3+}离子密度

D^{+}离子密度

How the capsule imperfections affect the ICF implosion performance?

- The shock-induced kinetic effect enhances the ion mixing, causing the ‘mixed’ area to increase faster over time than diffusion.
- The viscosity of the post-shock nonuniform plasmas is ~2 times higher than that of the post-shock uniform carbon plasma.

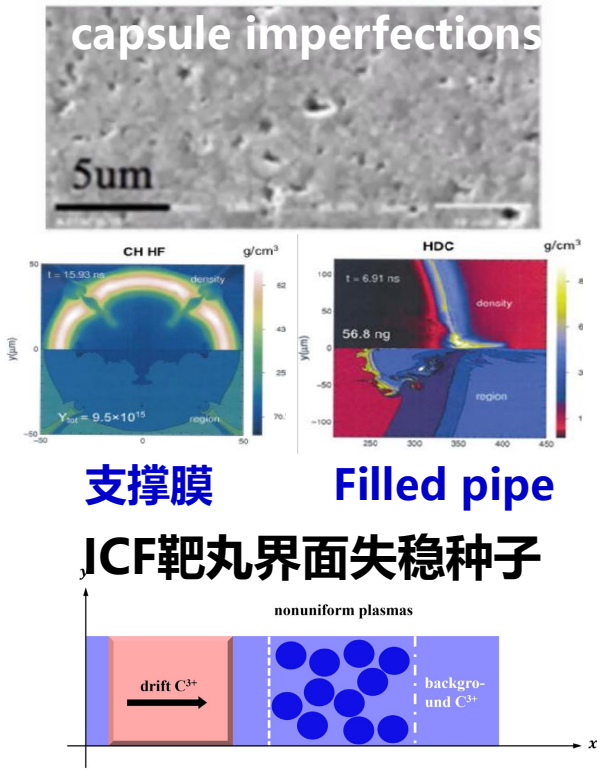

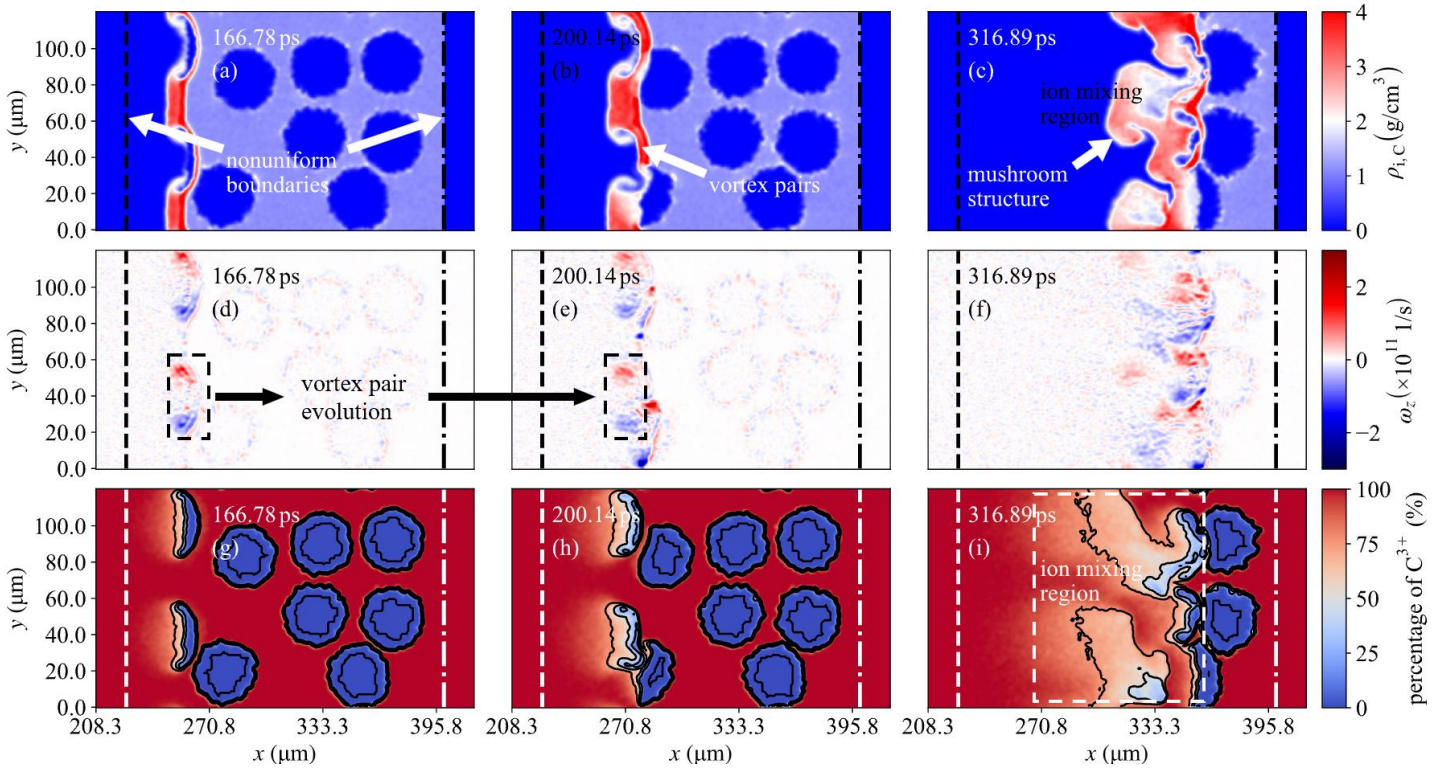

Hybrid simulation

涡强度

C³⁺数密度占比

[1] F.Q. Meng et al.， Hybrid simulation of shock interaction with highly nonuniform plasmas, New Journal of Physics, 26 063039 (2024)

[2] F.Q. Meng et al.， Hybrid simulation of shock-bubble interaction in multi-species plasmas, PPCF 67, 085014 (2025)

北京应用物理与计算数学研究所
Institute of Applied Physics and Computational Mathematics

三、等离子体中冲击波对撞：黑腔动力学场景

3.1 相向运动冲击波对撞过程中的非平衡动理学效应

冲击波对撞过程中，产生了较强静电波状结构，导致了高温高密度平台和10keV高能离子的出现，影响ICF黑腔的性能

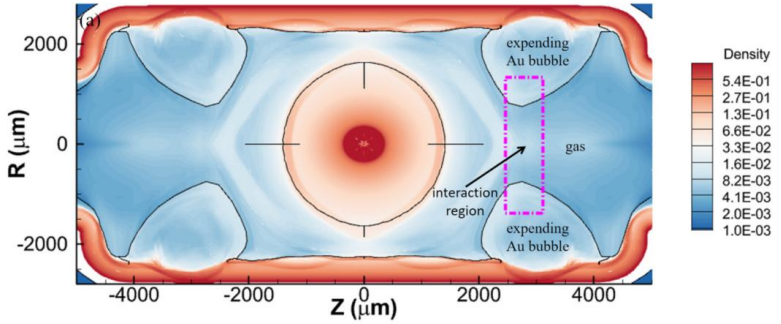

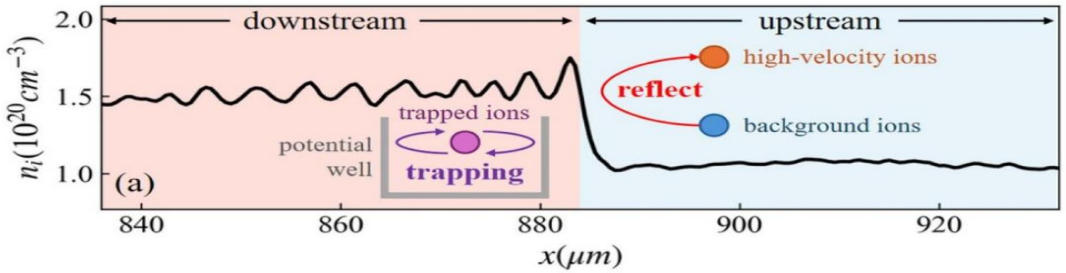

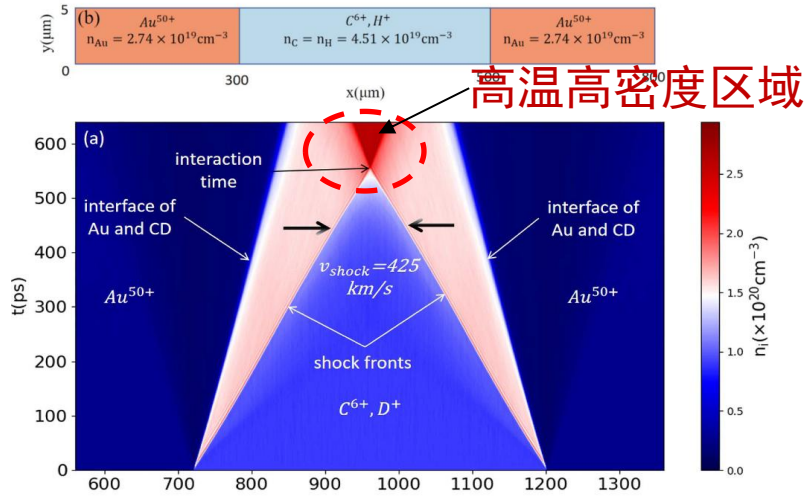

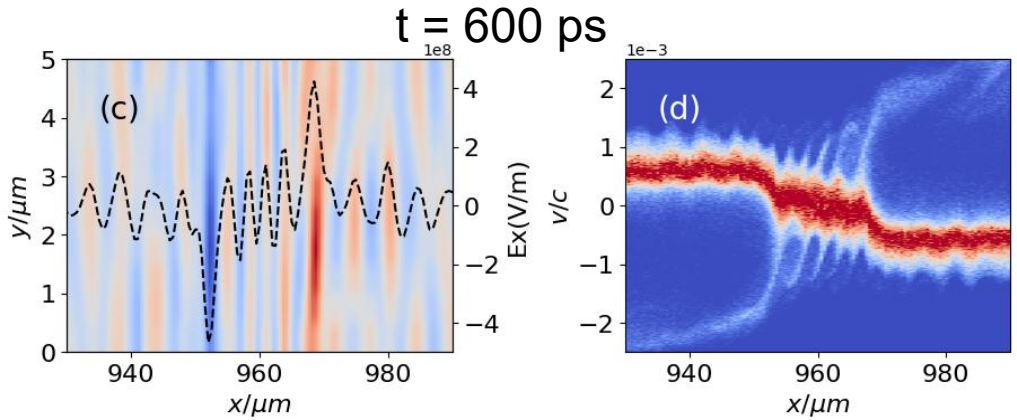

存在波和高能离子，黑腔“能量丢失”

[1] 张旭 等，Kinetic effects on the interaction of counter-propagating plasma shocks inside an ICF hohlraum, Nucl. Fusion 64, 096005 (2024).

三、等离子体中冲击波对撞：黑腔动力学场景

3.2 相向运动冲击波对撞过程中的非平衡动理学效应

冲击波对撞会产生稳定的密度平台，其密度低于流体预测且存在离子混合，降低ICF黑腔中LPI的预测精准度 （红移）

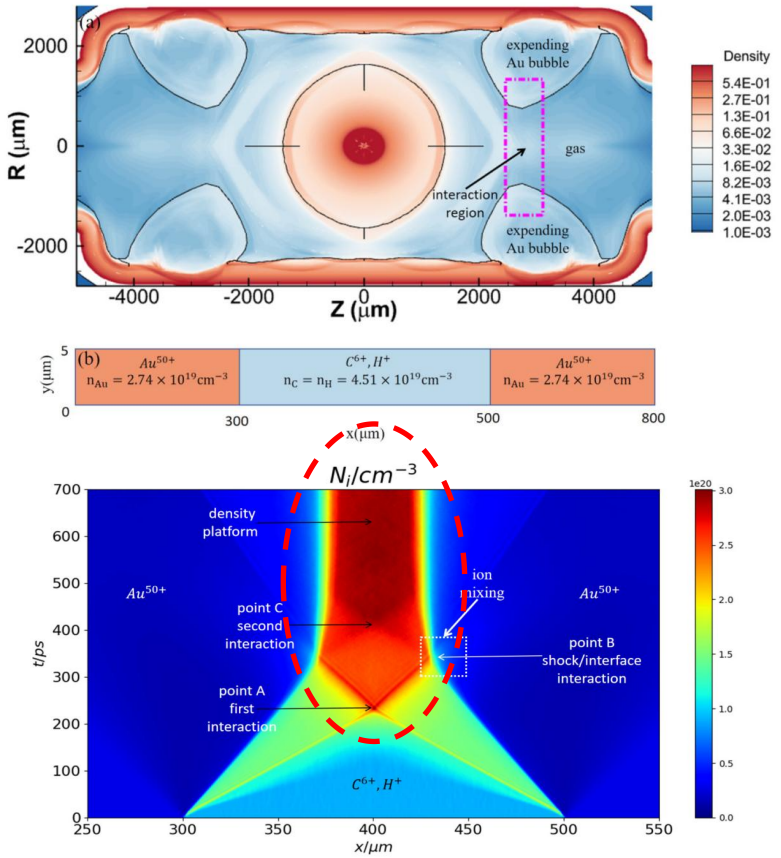

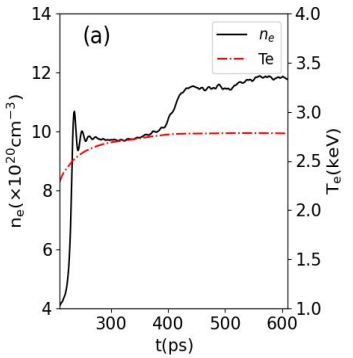

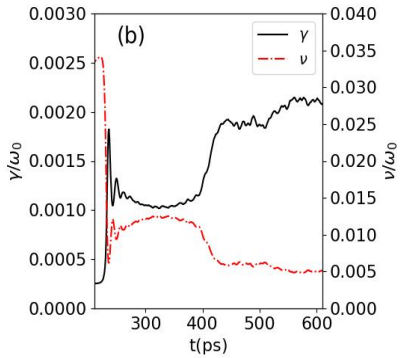

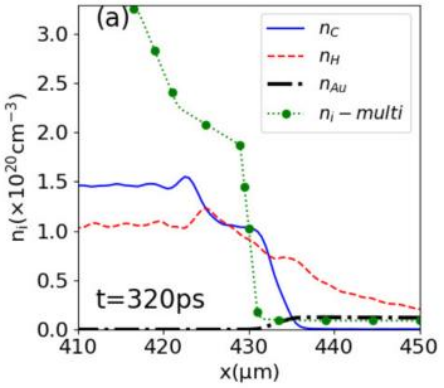

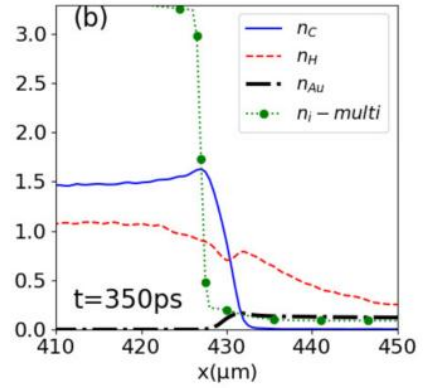

SRS散射光波长与密度紧相关，可解释ICF实验SRS光谱红移

$$\frac{\lambda_0}{\lambda_s} = 1 - \left(\frac{1}{n_{cr}} \left[\frac{\omega_0^2}{c^2} \frac{3 k_B T_e}{\pi e^2} \left(1 - \frac{n}{n_{cr}} \right) \times \left(1 - \sqrt{\frac{n}{n_{cr}}} + \frac{1}{4} \frac{n}{n_{cr}} \right) + n \right] \right)^{\frac{1}{2}},$$

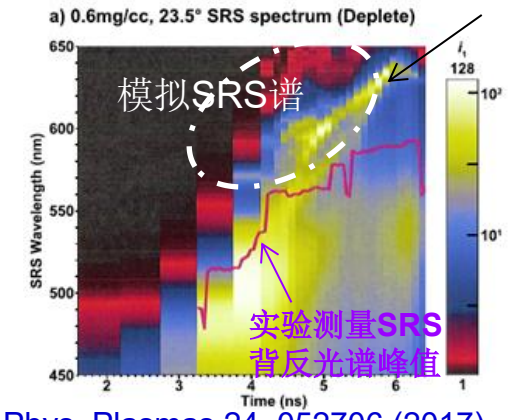

红移

Phys. Plasmas 24, 052706 (2017)

[2] 张旭 等，Large time-scale kinetic simulations of counter-propagating plasma shocks in the hohlraum, PPCF, 67, 115001 (2025) .

To elucidate the influence of ion mixing on the evolution of RMI with greater clarity, shock waves with different Mach numbers were employed

- With stronger shocks producing larger ion mixing region. Interface mixing can be modeled either as a reduction factor or as an enhanced viscosity, leading to suppression of the instability amplitude growth.
- We see energetic ions induce an anomalously diffusive mixing layer at the interface and preheat the material ahead of the shocks. Where these energetic ions from?

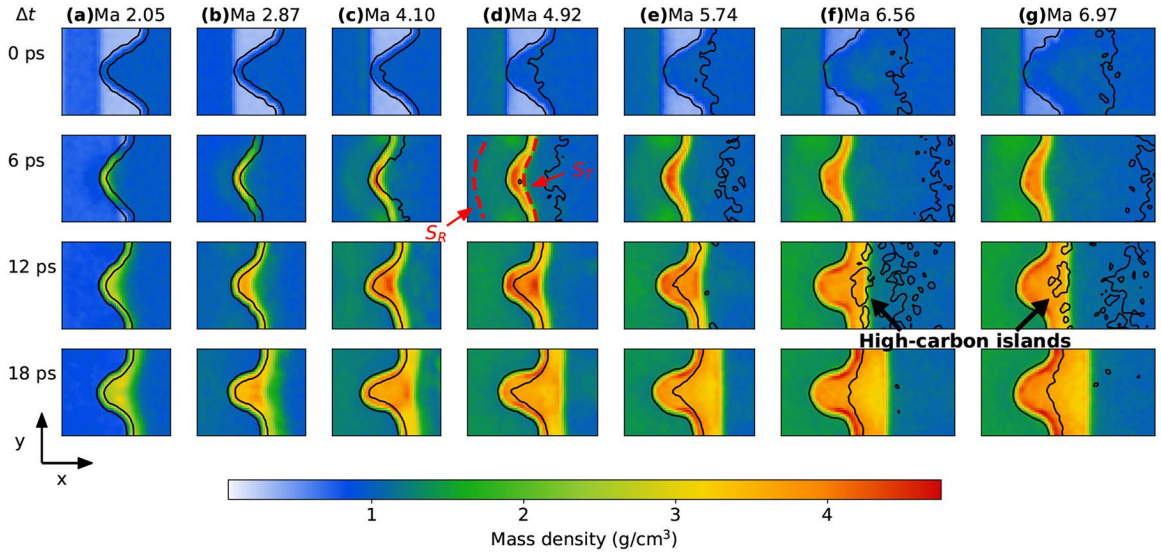

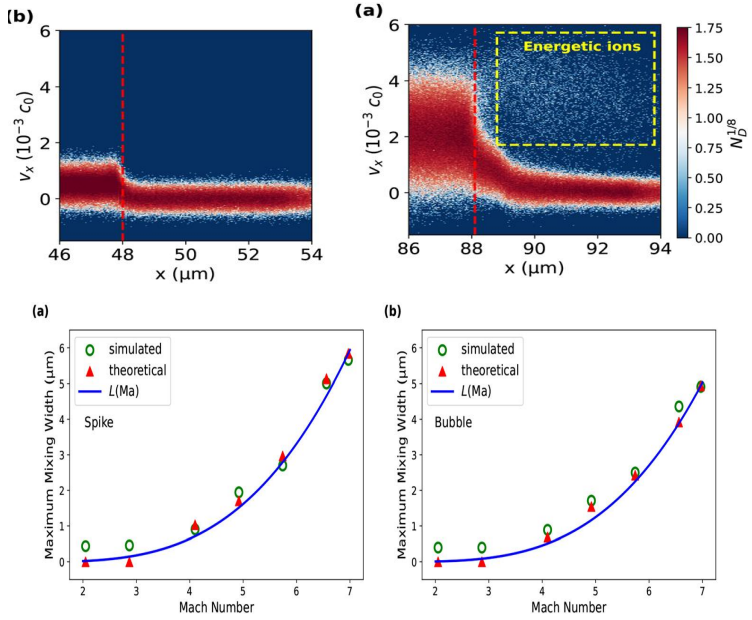

[1] Z.H. Lin et al., The effects of energetic ions in light/heavy Richtmyer–Meshkov instability, Phys. Plasmas 32, 082111 (2025)